Miner Petrol (2017) 111:435–457
DOI 10.1007/s00710-017-0509-z

ORIGINAL PAPER

Zircon and whole-rock Zr/Hf ratios as markers of the evolution of granitic magmas: Examples from the Teplice caldera (Czech Republic/Germany)

Karel Breiter[1] · **Radek Škoda**[2]

Received: 23 September 2016 / Accepted: 17 March 2017 / Published online: 29 March 2017

Abstract Hafnium contents and Zr/Hf ratios were studied in zircons and their parent rocks from three magmatic suites associated with the Teplice caldera, Eastern Erzgebirge: rhyolite and dacite from the peraluminous Schönfeld Unit, relatively younger A-type Teplice rhyolite, and post-caldera A-type biotite and zinnwaldite granite and greisen. New data suggest that zircon crystallizing from a geochemically less evolved volatile- and water-poor melt is, compared to the host rock, relatively Hf-depleted, while zircon crystallizing from an evolved volatile- and water-rich melt has a Zr/Hf value approximately identical to that of the parental melt. Zr/Hf values in zircon did not change substantially either during greisenization, or during low-temperature alteration after metamictization. Zr/Hf values in the whole rock may serve as a sensitive indicator of magmatic fractionation of evolved granitic melts, as they are only negligibly influenced by the following hydrothermal processes. Zr/Hf values in individual cogenetic zircon grains are scattered but their general evolution trend in the rock series is consistent with the evolution of the whole-rock Zr/Hf values.

Keywords Zr/Hf value · Zircon · Teplice caldera · Rhyolite · Rare-metal granite · Cínovec deposit

Editorial handling: L. Nasdala

✉ Karel Breiter
breiter@gli.cas.cz

[1] Institute of Geology of the Czech Academy of Sciences, v.v.i., Rozvojová 269, CZ-165 00 Praha 6, Czech Republic

[2] Department of Geology, Masaryk University, Kotlářská 2, CZ-611 37 Brno, Czech Republic

Introduction

Zirconium (Z = 40) and hafnium (Z = 72) are elements of group 4b of the Periodic Table, have similar ionic radii (0.84 and 0.83 Å, respectively, in eightfold coordination, Shannon 1976) and are quadrivalent under all geological circumstances. Consequently, the crystal chemical properties of both elements are very similar, and the Zr/Hf value remains constant during the majority of geological processes (Hanchar and Hoskin 2003). Wang et al. (2010) summarized literature data for 2200 electron probe analyses of granitic zircon and found a median of 1.48 wt% HfO_2. They also reported that the Zr/Hf value (by weight) is in the range of 37–38, i.e., slightly higher than the value proposed for the whole Solar System (Zr/Hf = 34.1 ± 0.3 by weight) by Patzer et al. (2010). Pupin (2000) reported the results of 9000 electron probe analyses of magmatic zircon and found a decrease in the Zr/Hf median value from 60–70 in mantle-derived plagiogranites, hypersolvus alkali granites and alkali syenites, to 40–45 in hybrid calc-alkaline granitoids, and finally to 35–37 in peraluminous granites and migmatites.

Belousova et al. (2002) provided 656 LA-ICP MS and electron probe analyses of zircon from rocks ranging from kimberlites through basalts and granitoids to alkali syenites and found 0.7–2.7 wt% HfO_2 with an enormous variation in each rock type. Nevertheless, the medians were found to increase from syenites and basalts (0.70 and 0.72 wt%, respectively) through lamproites, alkali syenites and carbonatites (1.17, 1.22 and 1.23 wt%, respectively) to granitoids and kimberlites (1.51 and 1.55 wt% HfO_2, respectively). Rubatto (2002) reported approximately 9000–12,000 ppm Hf (ca. 1.1–1.4 wt% HfO_2) in zircons from granulites and eclogites. Grimes et al. (2015) found 7000–17,000 ppm Hf (ca. 0.8–2.0 wt% HfO_2) in zircons from mid-ocean ridge basalts, continental arcs and post-collisional granitoids, without a

statistically significant difference between particular tectono-magmatic sources. All these data indicate that the Zr/Hf values in zircon from the upper crust resemble those of the whole Solar System, while zircon from the majority of mantle-derived rock is Hf-depleted. Some increase in the Hf content in zircon along with the fractionation of a composite granitoid pluton was noted from the McMurry Meadow pluton, California (Sawka 1988), the Sweetwater Wash pluton, California (Wark and Miller 1993), Boggy Plain pluton (Hoskin et al. 2000), and Spirit Mts. batholith, Nevada (Claiborne et al. 2006).

In contrast to the above mentioned rock types, a strong enrichment in Hf – thus a decrease in the Zr/Hf values in zircon – was noted in many fractionated granites and pegmatites (Tab. 1). Cheng et al. (1992) reported zircon with up to 18.7 wt% HfO_2, i.e., Zr/Hf = 2.2 by weight, from the Beauvoir granite, France. Wang et al. (2000) found a decrease in the Zr/Hf values in zircon from 30–95 in biotite I-type granites through 7–52 in A-type alkali granites to 3.9–38 in arfvedsonite granites (with a max. 12.37 wt% HfO_2) in Laoshan, eastern China. In Cornwall, the Zr/Hf values in zircon decreased from 50–110 in biotite and tourmaline granites to 6–80 in the most evolved topaz granites (Meldon Aplite and Megiliggar Rocks, Breiter et al. 2016). A strong increase in the Hf contents in zircons in fractionated rare metal granite systems was noted from Suzhou (A-type, China, Wang et al. 1996), Yichun granite (S-type, China, Huang et al. 2002), Beauvoir (S-type granite) and Cínovec (A-type, Czech Republic/Germany, Breiter and Škoda 2012). An increase in the HfO_2 contents in hafnian zircon during the evolution of the Tanco pegmatite was reported by Van Lichtervelde et al. (2009). An evolution from Hf-rich zircon to hafnon, $HfSiO_4$, was reported from LCT-type pegmatite of Koktokay, China (Yin et al. 2013).

A decrease in the Zr/Hf ratios was registered not only within a magmatic suite but also within individual zircon crystals. Hf enrichment of the zircon rim compared to its core was reported for example from several granite plutons in Japan (Hoshino et al. 2010) and from granites in Elba, Italy (Gagnevin et al. 2010). It was confirmed as a common feature of zircon crystals from some A-type rare-metal granites (Breiter et al. 2014).

In the whole rock, the proposed Zr and Hf abundances increased from 3.6 and 0.106 ppm in the C1 chondrite (Lodders 2010) through 10.8 and 0.3 ppm in the mantle (Palme and O'Neill 2004) to 190 and 5.8 ppm in the upper continental crust (Taylor and McLennan 1995), respectively. This, with respect to a high uncertainty of all these values, gives a nearly constant Zr/Hf value in the range of 35–40. In other words, there is very small, if any, Zr/Hf fractionation among primordial Earth, mantle and common crustal rocks including calc-alkaline granites.

It was a general consensus that the whole-rock Zr/Hf values remain stable in comagmatic suites (Lyakhovich and Shevaleevskii 1962; Kosterin et al. 1963; Broska et al. 1990). This is probably valid in basic, intermediate and poorly evolved granitic rocks. For example, in the Bohemian Massif, the majority of Paleozoic granitoids including Cambrian/Ordovician granites and orthogneisses, Variscan I-type granites of the Central Bohemian pluton, Variscan two-mica granites of the Moldanubian (South Bohemian) pluton and Variscan S-type biotite granites in the Erzgebirge, show Zr/Hf values over a narrow range of 24–35 (with several outliers to 41, unpublished authors data), i.e., similar to, or only slightly lower than, the Solar value of 34. In contrast, a systematic decrease in Zr/Hf values during fractionation was reported from rare-metal granite suites (RMG, Table 1), such as the Beauvoir granite (from 17 to 6.4, Raimbault et al. 1995), Fichtelgebirge pluton, Germany (38 → 25, Irber 1999), Podlesí stock in Western Erzgebirge (from 21 to 9, Breiter et al. 2005), Land s End pluton, Cornwall (from 41 to 19, Müller et al. 2006) and Akchatau, Kazakhstan and Kukulbei, Transbaikalia (both Zaraisky et al. 2009). Similar processes should be expected in complex pegmatites but appropriate whole-rock data are missing.

The origin of Zr/Hf fractionation in RMG and pegmatites was explained by magmatic fractionation (e.g., Wang et al. 1996, 2000). Later, Kempe et al. (2000) questioned magmatic fractionation and proposed the origin of Hf-rich zircon from F-rich fluids associated with albitization. Furthermore, Johan and Johan (2005) explained the origin of the Hf-enriched rims of zircon crystals from Cínovec as a product of postmagmatic fluid-related fluorination. This view was supported by experimentally constrained fluid–melt distribution coefficients for Zr and Hf (London et al. 1988), which indicated a higher activity of Hf in fluids associated with a peraluminous melt. Nevertheless, Linnen and Keppler (2002) experimentally demonstrated a systematic decrease in Zr/Hf values in fractionated metaluminous and peraluminous melts and an increase in Hf contents in crystallizing zircon, i.e., the possibility of fully magmatic origin of Hf-rich zircon. Finally, Zaraisky et al. (2009) experimentally determined a difference in the Zr/Hf value between zircon and metaluminous and peraluminous melts with different contents of fluorine as follows: all experiments revealed that $Zr/Hf_{zircon} > Zr/Hf_{melt}$, i.e., the residual melt (and later population/zones of zircon) will be systematically enriched in Hf.

Altogether, there exist satisfactory literature accounts regarding Hf contents and Zr/Hf ratios in both mineral zircon and whole-rock granitoids, and the Zr/Hf value is considered to be a reliable indicator of the evolution of fractionated magmatic suites (Hoskin and Schaltegger 2003; Zaraisky et al. 2009). However, surprisingly, there is only poor knowledge about the relationship between the Zr/Hf ratios in zircon and those in its parental rock. Only Claiborne et al. (2006) reported

Table 1 HfO_2 contents and Zr/Hf values of zircon from strongly fractionated granites/pegmatites and Zr/Hf values of their host rocks (if available)

Area	Rock type	Rock Zr/Hf (by weight)	Zircon HfO_2 (wt%)	Zircon Zr/Hf (by weight)	Reference, remarks
Beauvoir, France	Strongly fractionated peraluminous granites		2.5 → 18.7	20 → 2.2	Cheng et al. (1992)
			2 → 19	23 → 2	Breiter and Škoda (2012)
		17 → 6.4			Raimbault et al. (1995)
Cornwall, GB	Biotite and tourmaline granites	31–37	1–2.2	50–110	Chappel and Hine (2006); Breiter et al. (2016)
	Topaz granites	11–23	1.5–7	6–80	Breiter et al. (2016); Breiter unpublished WR data
Suzhou, China	Fractionated A-type granites	8.1 → 2.4	2 → 34	30 → 1	Wang et al. (1996)
Yichun, China	Lepidolite granite	5–7	4.5–22	1.7–9.5	Huang et al. (2002)
Laoshan, China	I-type granites		0.6–1.9	30–95	Wang et al. (2000)
	A-type alkali granites		1.1–7	7–52	
	Arfvedsonite granites		1.5–12.4	3.9–38	
Krušné Hory/Erzgebirge, Czech Republic/ Germany	Peraluminous less-fractionated biotite granites	34–39	0.8–2.0	27–55	Breiter et al. (2005); Breiter and Škoda (2012); Breiter and Škoda, this work; Breiter, unpublished data
	Peraluminous more fractionated biotite granites	16–31	1–4	16–54	
	Peraluminous zinnwaldite granites	9–21	0.9–8	5–45	
	A-type biotite granites	16–24	1 → 4.5	55 → 10	
	A-type zinnwaldite granites, different facies	16 → 4.5	2 → 12	23 → 3.3	
	Peraluminous rhyolite and dacite	30–39	0.75–2.1	21–56	
	A-type rhyolite and granite porphyry	17–39	0.8–3.2	13–57	
Moldanubian pluton, Czech Republic/Austria	Two-mica granites	24–35	1.0–1.8	30–58	Breiter (2016)
Tanco, Canada	LCT pegmatite		7.7 → 24.8	5.6 → 1.6	Van Lichtervelde et al. (2009)
Koktokay, China	LCT pegmatite		4.2 → 58.9	13 → 0.17	Yin et al. (2013) (transition from zircon to hafnon)

x–y, the value scattered between x and y; x → y, the value generally evolved from x to y

a notable decrease in the whole-rock (WR) and zircon Zr/Hf values during the evolution of the Spirit Mountain batholith, Nevada; the Zr/Hf values in zircon were systematically higher than those in the host granite. Later Erdmann et al. (2013) mentioned two coexisting populations of zircon in the Nunavut granite in Canada: the older population had a higher Zr/Hf ratio and the younger population had a lower Zr/Hf ratio than the parental rock.

We decided to fill this gap in this article, aiming (i) to define the evolution of HfO_2 contents and Zr/Hf ratios in fractionated granitic intrusive and volcanic suites, (ii) to compare the Zr/Hf values in zircon and its parental rocks of different geochemical affiliations and grades of fractionation; and (iii) to evaluate the possible use of Zr/Hf values for the interpretation of rare-metal granite systems. The Teplice caldera in the Eastern Erzgebirge seems to be an ideal object for such a study; here, two deep boreholes allow to study vertical evolution of zircon and its parental rock in two volcanic suites (S-type Schönfeld rhyolite and dacite followed by A-type Teplice rhyolite) and a suite of rare-metal Cínovec granite (A-type). Preliminary data on zircon from the Teplice rhyolite (Breiter and Škoda 2009) were complemented by new zircon and WR data from all volcanic rocks (Table 2). Vertical variations in the composition of zircon in granites from borehole CS-1 have been reported by Breiter and Škoda (2012), and WR data have been reported by Breiter et al. (in review). Here, we extend our attention to zircons from the greisen and minor, but genetically important, granite facies (Table 3) and their comparison with the whole-rock Zr/Hf values.

Geological setting and samples

Late Variscan granites and associated acidic volcanic rocks of the Krušné Hory/Erzgebirge form a ca. 80 km long NE–SW-oriented belt, which intruded into the Variscan crystalline complex (mainly Neoproterozoic to Early Paleozoic metapelites and metagranitoids) of the Saxo-Thuringian domain in the NW part of the Bohemian Massif (Hoth et al. 1995; Förster et al. 1999; Cháb et al. 2010; Linnemann and Romer 2010) in a relatively short period from ~330 to 310 Ma (Förster and Romer 2010; Ackerman et al. 2016). The

Table 2 Stratigraphy of the Teplice caldera fill (borehole Mi-4, according to Breiter et al. 2001) with a list of the studied zircon samples

Depth (m)	Unit	Description	Samples
Not in borehole, samples obtained from outcrops	Granite porphyry GP	Coarse porphyritic (Kfs, bipyramidal Qtz) dyke rock with fine-grained granitic matrix	3531, 3532, 3533
0–191.4	Teplice rhyolite TR3	Fine-grained rhyolite ignimbrite with 35 vol% of phenocryst (Kfs)	3194, 3198
Weathered surface			
191.4–490.6	Teplice rhyolite TR2	Tuffs with lava clots changed upwards to ignimbrite, content of phenocryts varied from 30 to 50 vol% (Qtz, sanidine, Ab)	3200, 3201, 3203, 3205
Sedimentary layer, shale, coal			
493.4–601.6	Teplice rhyolite TR1	Rhyolitic tuff and ignimbrite with 30 vol% of phenocrysts (Qtz, sanidine, Ab)	3208, 3210
Sedimentary layer, shale, coal			
604.3–868.3	Schönfeld dacite DC	Dacitic tuffs and ignimbrites with 25 vol% of phenocrysts (oligoclase, Bt) and lithic fragments	3211, 3216
Sedimentary layer, arcose, shale, coal			
870.1–924.5	Schönfeld basal rhyolite BR	Rhyolite tuffs of ash flows with 30 vol% of phenocrysts (Qtz, sanidine, Ab, Bt)	3219, 3220

following two types of magma were generated and emplaced synchronously during this event (Breiter 2012): (1) strongly peraluminous P-rich (S-type) melts dominating the western and central parts of the Erzgebirge, and (2) slightly peraluminous P-poor melts (A-type), forming both intrusive and volcanic rocks mainly in the eastern part of the area. Both magmatic suites culminated with strongly fractionated subvolcanic granite intrusions followed by Sn + W ± Li-Nb-Ta mineralization of the greisen type.

The dominant geological structure of the Eastern Erzgebirge is the Teplice caldera with a size of approximately 40 × 20 km (Fig. 1). A detailed knowledge of its stratigraphy (Breiter 1997; Breiter et al. 2001 and references therein) permits the establishment of the sequence of Variscan magmatic events in the Eastern Erzgebirge as follows:

Step 1– intrusion of peraluminous biotite granites (Fláje and Telnice plutons in Bohemia, Niederbobritsch in Saxony);

Step 2– eruption of peraluminous rhyolite and dacite lavas and tuffs with sedimentary intercalations (so-called Schönfeld Unit) at Schönfeld (Saxony) and Mikulov (Bohemia);

Step 3– three stages of sub-aluminous rhyolite volcanism of the A type ("Teplice rhyolite"), gradually passing from explosive to effusive in nature;

Table 3 A vertical section through the Cínovec granite cupola (borehole CS-1, according to Breiter et al. in review) with a list of the zircon samples studied

Depth (m)	Unit (symbol)	Description	Samples
0–284	Zinnwaldite granite of the canopy of the cupola (ZiGc)	Fine-to-medium grained zinnwaldite granite, locally albitized, sericitized or kaolinized	4672, 4674, 4677, 4678, 4680, 4683, 4685
Individual bodies (range 39–199)	Greisen bodies (GR)	Quartz-zinnwaldite greisen with topaz, fluorite, cassiterite, wolframite, columbite and scheelite	4971, 4972, 4974, CS1/10
284–369	Mica-free granite with feldspatite intercalations (MfG)	Medium-grained quartz-albite-Kfs granite with variable Ab/Kfs-ratio	4686, 4932, 4933
369–521	Zone of rafts of zinnwaldite microgranite (ZiGm)	Porphyritic (bipyramidal Qtz, Kfs) fine-grained zinnwaldite granite	4687
521–735	Main body of the zinnwaldite granite (ZiG)	Medium-grained zinnwaldite granite	4688, 4689, 4800
735–1597	Biotite granite (BtG)	Biotite granites with variable texture (fine-grained porphyritic to coarse-grained equigranular)	4690, 4691, 4692, 4693, 4801, 4802, 4803
Southern part of the deposit, samples from the old mine	Granite of the canopy of the cupola	Fine-to-medium grained zinnwaldite granite	5434, 5436
	Greisen bodies	Quartz-zinnwaldite greisen with topaz, fluorite, cassiterite, wolframite, columbite and scheelite	6, 7, 10, 20, 5427, 5428

Step 4– collapse of the rhyolite volcano and creation of the Teplice caldera;
Step 5– intrusion of ring dykes of granite porphyry;
Step 6– intrusion of biotite granites of the A-type without hydrothermal activity (Preiselberg body in Bohemia, Schellerhau body in Saxony);
Step 7– intrusion of strongly fractionated ore-bearing granite of the A-type in several pulses (biotite and zinnwaldite granites at Cínovec and several other localities).

Two deep boreholes realized between 1960 and 1985 provide a good opportunity to study the magmatic evolution of volcanic and subvolcanic rocks of the caldera and vertical differentiation of the post-caldera rare-metal granites. Borehole Mi-4 at the village of Mikulov (Figs. 1 and 2) was 1200 m deep and penetrated the volcanic fill of the caldera in the interval 0–924.5 m. The oldest member of the caldera fill, the Schönfeld Unit, consists of basal rhyolite (BR, 71–73 wt% SiO_2) at the depths ranging from 924.5 to 868.3 m and of dacite (DC, 61–67 wt% SiO_2) at the depths ranging from 868.3 to 609.6 m. It can be classified as a slightly peraluminous calc-alkaline (S-type) rock similar to common granitoids of the "older intrusive complex" of the Erzgebirge (sensu Tischendorf 1989). The basal rhyolite shows a slight increase in Si and a decrease in Ti, Mg, Nb, Y and REE in upwards direction, while the dacite shows an opposite trend.

The subaluminous (A-type, 75–77 wt% SiO_2) "Teplice rhyolite" extends from the depth of 609.6 m to the actual surface. Within this profile, three distinct units were recognized – TR1 at a depth of 609.6–490.6 m, TR2 at a depth of 490.6–191.4 m, and TR3 at a depth of 191.4 m to the actual surface. All TR units show reversed vertical differentiation of trace elements, i.e., starting with relatively Rb-, Nb-, Th-, and Y-rich and Ti-, Sr-, Zr-, and Ce-poor basal parts, passing gradually upwards to a less acidic Rb-, Nb-, Th-, and Y-poor and Ti-, Sr-, Zr-, and Ce-rich upper part (details in Breiter 1997). Ring dykes of granite porphyry (Fig. 1, not recorded in borehole Mi-4) represent the latest cumulate-rich portion of rhyolite magma (Breiter 1997; Müller et al. 2005). Twelve samples of zircon and 29 whole-rock samples were analyzed from this borehole (Table 2). Additionally, three samples of granite porphyry from the outcrops of the ring dykes were analyzed.

Borehole CS-1 (Figs. 1 and 2) was drilled to a depth of 1596 m in the center of the Cínovec granite cupola from 1960 to 1962 to study the structure of the pluton subjacent to the actually mined Sn-W deposit (Štemprok and Šulcek 1969). Zinnwaldite granite sensu *lato* (hereafter ZiG) was shown to exist in several textural and mineral varieties to the depth of 735 m, and biotite granite (BtG) continues at greater depths (Table 3). Geochemically, the Cínovec BtG is evolved, slightly peraluminous P-poor A-type granite, while the comagmatic ZiG is even more strongly enriched in F, Li, Rb, Zr, Th, HREE, Sc, Sn, W, Nb and Ta, and depleted in P, Ti, Mg, Ca, Ba and Sr. Whereas the BtG is chemically generally homogeneous, the ZiG underwent a strong differentiation with upwards increasing contents of LILE and rare elements (Breiter 2012). Twenty samples of zircon from borehole CS-1 and another 6 from the southern part of the Cínovec cupola were analyzed (Table 3). For the evaluation of the whole-rock Zr/Hf values, 254 chemical analyses from a previous study (Breiter et al. in review) were exploited.

Analytical methods

Zircon grains were studied in polished thin sections. Back-scattered electron (BSE) images were obtained on a TESCAN scanning electron microscope housed in the Institute of Geology CAS in Praha before the study of internal zoning of the individual zircon grains and their relative position to rock-forming minerals (Fig. 3).

Elemental abundances of W, P, As, Nb, Ta, Si, Ti, Zr, Hf, Th, U, Y, La, Ce, Pr, Nd, Sm, Gd, Dy, Er, Yb, Al, Sc, Bi, Mn, Fe, Ca, Pb, Mg, S, and F in zircon were determined using a CAMECA SX100 electron probe microanalyser (EPMA, Masaryk University and Czech Geological Survey, Brno) in wavelength dispersion mode. Zircon was analyzed at an accelerating voltage and beam current of 15 keV and 40 nA, respectively, and with a beam diameter ranging from 1 to 2 μm. The following reference materials were used: Ca – fluoroapatite, La – $LaPO_4$, Ce–$CePO_4$, Pr – $PrPO_4$, Nd – $NdPO_4$, Sm – $SmPO_4$, Gd – $GdPO_4$, Dy – $DyPO_4$, Er – $ErPO_4$, Yb – $YbPO_4$, U – metallic U, Th – $CaTh(PO_4)_2$, Pb – vanadinite, Zr and Si – zircon, As – lammerite, Y – YAG, Hf – metallic Hf, Mn – Mn_2SiO_4, Fe – almandine, Al – gahnite, S – $SrSO_4$, F – topaz, Sc – $ScVO_4$, Ti – titanite, Nb – columbite from Ivigtut, Ta – $CrTa_2O_6$, W – metallic W, Bi – metallic Bi, Mg – $MgAl_2O_4$. Raw data were processed using the X-Phi matrix correction routine of Merlet (1994). Empirically determined correction factors were applied to the overlapping X-ray lines. Empirical formulae of zircon were calculated on the basis of 4 atoms of oxygen in a formula unit (4 O *apfu*).

The WR major element analyses (wet technique) were performed at the Czech Geological Survey, Praha. The weights of the analyzed samples were 2–4 kg. Replicate analyses of the international reference material (JG-3 granodiorite; Geological Survey of Japan) yielded an average error (1 σ) of ±1% with respect to the recommended values (Govindaraju 1994). Trace elements were determined by ICP mass spectrometry following lithium metaborate/tetraborate fusion of a 0.2 g sample in the laboratory of ACME, Vancouver, Canada. (Details can be found at http://acmelab.com/.)

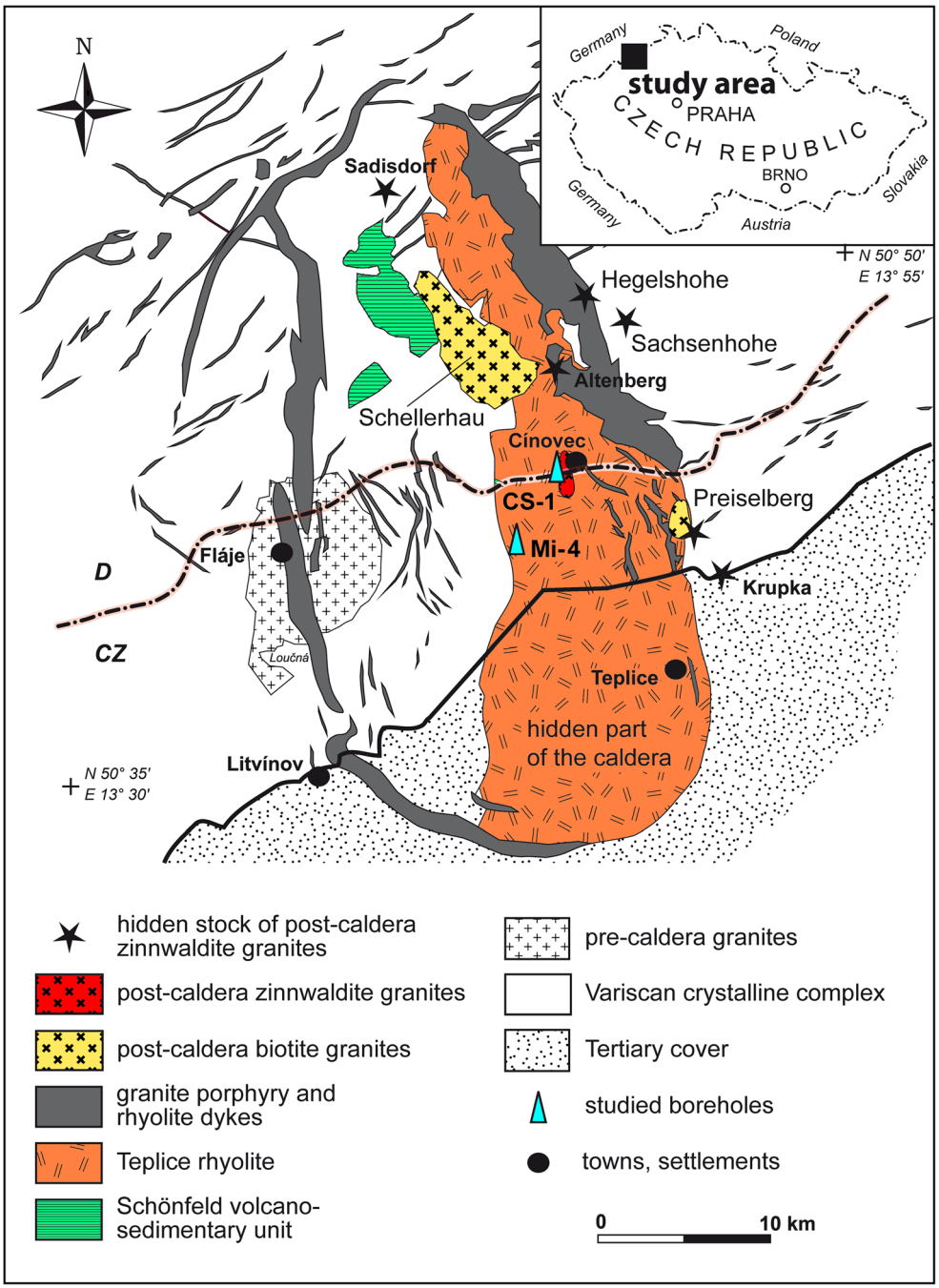

Fig. 1 Geological sketch of the Teplice caldera

Results

Zircon shapes

Zircon in the Schönfeld rhyolite (Fig. 3a) and dacite (Fig. 3b, c) forms mostly homogeneous or slightly zoned isometric to long columnar crystals 30–120 μm in size, sometimes with inclusions of glassy matrix. Bright inner zones are relatively slightly enriched in Y and U. Occasionally, a very subtle Hf enrichment from the core to the rim was found. Isometric oscillatory zoned grains were found only rarely.

Zircon in the Teplice rhyolite mostly forms euhedral, isometric to shortly columnar crystals 20–100 μm, rarely up to 400 μm in size. In all samples, oscillatory zoned grains (Fig. 3d) are associated with grains showing patchy-zoned (metamictized) cores and more regular rims (Fig. 3e, f). The bright rim of the crystal in Fig. 3f is enriched in Y, Th and U, while bright rim of the crystal in Fig. 3e is slightly enriched in Hf. Zircon in granite porphyry usually forms homogeneous, shortly columnar crystals 40–150 μm in size or their fragments. Occasionally, grains have patchy cores and more regularly zoned rims (Fig. 3g). Some grains contain numerous inclusions of glassy groundmass.

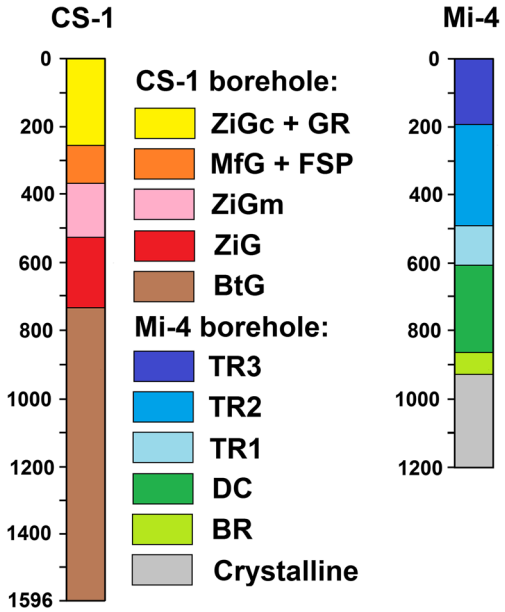

Fig. 2 Simplified sections through the caldera fill in borehole Mi-4, and through the Cínovec granite cupola in borehole CS-1

Zircon crystals from the biotite granite from Cínovec are mostly 10–50 μm in size, enclosed in dark mica. They are often distinctly zoned and contain contrasting blebs of exsolved mineral phases close to xenotime and thorite in composition (Fig. 3h). Zircon associated with thorite is surrounded by a secondary halo of iron hydroxides (Fig. 3i). Zircon from the zinnwaldite granite features isometric crystals of similar sizes enclosed in quartz and feldspars, but some of the later crystallized grains occupy interstices between other minerals. Some of the crystals are irregularly zoned in BSE images and/or contain numerous tiny cavities (Fig. 3j). Thin rims of xenotime around zircon crystals (Fig. 3k) are common.

Zircon grains from the greisen, mica-free granite facies and feldspathite feature a maximum size of 120 μm and are texturally similar to those from the zinnwaldite granite. The internal composition is patchy, with domains enriched in Hf, Y and Th. In the few zoned grains, the cores are patchy and heterogeneous, porous and enriched in uranium, whereas the rims are compact, homogeneous and enriched in Hf. Epitaxis and overgrowth of xenotime on zircon is common (Fig. 3l, m). During the postmagmatic stage, zircon was usually stable when in contact with the ore-bearing fluid from which cassiterite and scheelite crystallized (Fig. 3n, o).

Chemical composition of zircon

Most published electron probe analyses of zircon included, besides major elements Si, Zr, and Hf, only the following other elements: U, Th, Y, P (Pupin 2000), and occasionally Ca, Al, Sc and Yb (Cheng et al. 1992; Johan and Johan 2005; Hoshino et al. 2010; Výravský et al. 2017 etc.). Trace element analyses provided by other methods like SHRIMP (Claiborne et al. 2006; Grimes et al. 2015) or LA-ICP-MS (Nardi et al. 2013) did not include major elements Si and Zr: the Zr/Hf values were derived from the assumption of an ideal occupation of the zircon crystal lattice. Data regarding the contents of Nb, Ta, W, As and F are generally sparse (Förster 2006; Van Lichtervelde et al. 2009; Förster et al. 2011; Breiter et al. 2006, 2009, 2014; Nb also Grimes et al. 2015).

We analyzed altogether 31 chemical elements in zircon, but to report all of them is beyond the scope of this paper. Below, we describe Hf contents and Zr/Hf values in detail, while other elements are commented only in the case of their unusually high contents. Complete analyses of typical zircon grains from all studied rocks are listed in Table 4. To meet both mineralogical and geochemical conventions, we refer to the contents of Hf and other minor elements and the Zr/Hf values in apfu in Fig. 4, while in all other figures these data are presented in weight units to be simply compared with the WR values. As a reminder, the solar and whole-Earth Zr/Hf value by weight equals 34 (Patzer et al. 2010).

In the calc-alkaline Schönfeld rhyolite, Hf contents in zircon varied in the interval of 0.75–2.1 wt% HfO_2 and the Zr/Hf value between 21 and 54 (median 41) (Fig. 5a), while in the comagmatic dacite 0.9–1.7 wt% HfO_2 and Zr/Hf = 26–56 (median 43) were found. The contents of other minor elements in zircon from both rocks are relatively low compared to those in other studied rock types: usually less than 1.5 wt% Y_2O_3, <1 wt% UO_2 and ThO_2 (Fig. 5b–d).

The chemical composition of zircon from the Teplice rhyolite was much more variable (Fig. 5a–d): 0.9–3.2 (median 1.4) wt% HfO_2 and Zr/Hf value by weight 13–57 (mostly between 20 and 40, median 32). Wide differences were found within the individual eruptive units. The Zr/Hf values increase clearly upwards from 31 to 42 within TR1, increase upwards with some variation from 33 to 38 in TR2, and slightly decrease upwards from 29 to 26 in TR3 (all values are medians). In the case of TR3, only the basal part of the whole unit has been preserved, and an unknown part has been eroded. The contents of other minor elements in zircon are higher than those in the Schönfeld unit and highly variable, mostly in the range of 0–5 wt% Y_2O_5, 0–2 wt% UO_2 and ThO_2, 0–1.5 wt% P_2O_5, 0–0.8 wt% F, occasionally up to 0.4 wt% As_2O_5 and 0.15 wt% Sc_2O_3. Many grains are obviously metamictized and altered, containing 2–4 (up to 8) wt% of non-formula element oxides Al_2O_3 + FeO + MnO + CaO. Analytical totals of such grains fall down to 90 wt%.

Granite porphyry representing the latest emplaced magma (remnants after extraction of previous rhyolite magmas of TR1–TR3) contains zircon grains with only 0.8–2.0 (median 1.4) wt% HfO_2 and Zr/Hf values of 21–55 (mostly 35–50, median 41). The Zr/Hf ratios in zircon in granite porphyry are thus higher than those in the youngest rhyolite unit TR3. The contents of minor and trace elements are the lowest of all

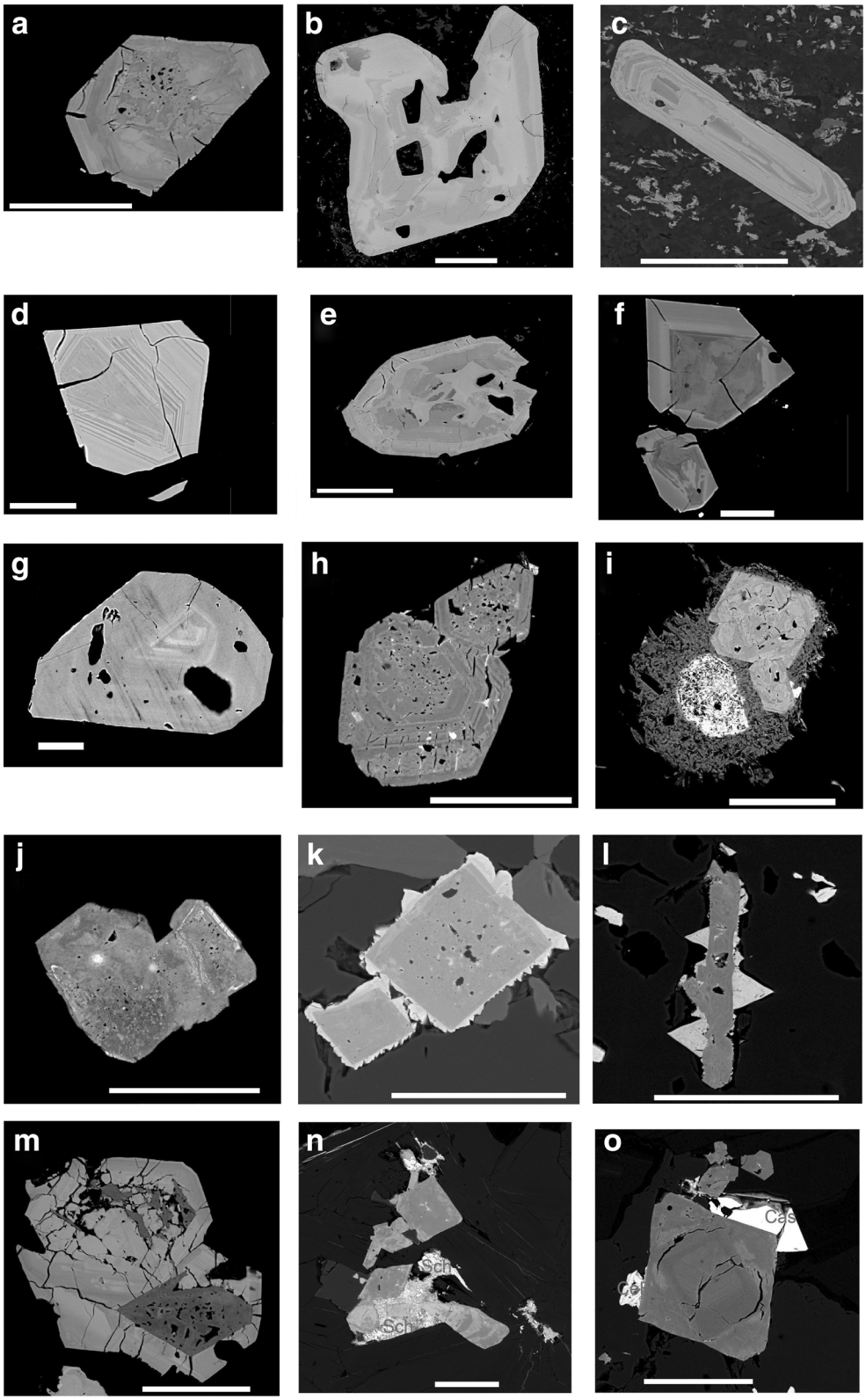

the studied rock types: <0.4 wt% Y_2O_3, <0.2 wt% ThO_2 and UO_2. Zircon from granite porphyry never shows metamictization-induced alteration, giving analytical totals >98 wt% in all cases.

Zircon from the Cínovec biotite granite is slightly more evolved than that from the Teplice rhyolite (Fig. 5e–h). It contains 1–4.5 (median 2.4) wt% HfO_2 and its Zr/Hf values are in the range of 10–55 (mostly 15–25, median 20). The

◀ **Fig. 3** BSE photomicrographs of zircon: **a**, zircon with a patchy core and a slightly zoned rim, basal rhyolite of the Schönfeld Unit, sample 3219, borehole Mi-4, depth of 897 m; **b,** an irregular, partly resorbed zircon grain with an inclusion of glassy matrix, sample 3212, dacite of the Schönfeld Unit, borehole Mi-4, depth of 637 m; **c,** columnar zoned zircon crystal, sample 3212, dacite of the Schönfeld Unit, borehole Mi-4, depth of 637 m; **d,** an oscillatory zoned zircon crystal, sample 3200, TR2 unit of the Teplice rhyolite, borehole Mi-4, depth of 234 m; **e,** a zircon grain with an irregular, patchy core and Hf-enriched rim, sample 3205, TR2 unit of the Teplice rhyolite, borehole Mi-4, depth of 443 m; **f,** a zircon grain with an irregular patchy core and Th, U, Y-enriched rim, sample 3208, TR1 unit of the Teplice rhyolite, borehole Mi-4, depth of 513 m; **g,** a slightly zoned crystal with inclusions of silicates, sample 3531, granite porphyry, outcrop at Loučná; **h,** two zircon crystals with mixed patchy and regular zoning, sample 4692, biotite granite, borehole CS-1, depth of 988 m; **i,** irregularly zoned zircon crystal (right up) in association with Ca, Th-fluorocarbonate (white), both rimmed by an Fe-oxide aggregate, sample 4692, biotite granite, borehole CS-1, depth of 988 m; **j,** irregularly patchy zoned Hf-rich zircon grain (bright areas are enriched in Y), sample 4672, zinnwaldite granite of the canopy, borehole CS-1, depth of 24.5 m; **k,** colander-like zircon crystal with a xenotime rim, zinnwaldite granite, sample 4688, borehole CS-1, depth of 559 m; **l,** a columnar zircon crystal with a xenotime epitaxis, quartz-zinnwaldite greisen, sample 4971, borehole CS-1, depth of 130 m; **m,** a colander-like zircon grain (dark gray) surrounded by zoned xenotime, quartz-zinnwaldite greisen, sample South 7, abandoned mine of Cínovec-south; **n,** zircon grains, some of them zoned, in association with scheelite (Sch), quartz-zinnwaldite greisen, sample CS1/10, borehole CS-1, depth of 53 m; **o,** a zircon crystal associated with cassiterite crystals (Cas) and a Ce-fluorocarbonate grain (CeF), quartz-zinnwaldite greisen, sample 4971, borehole CS-1, depth of 130 m. All scale bars are 50 μm

contents of minor elements are highly variable, mostly in the range of 0.5–2 wt% Y_2O_3, approximately 1 wt% UO_2 and less than 0.5 wt% ThO_2, but individual grains/zones containing several wt% of each of these oxides were found. Grains with unusually high Zr/Hf values (>30) are poor in U and Th, giving analytical totals of 97–100 wt%. As such, they probably did not undergo metamictization-induced alteration. Their low Hf contents seem to be a primary magmatic feature.

Zircons from the Cínovec zinnwaldite granite and greisen differ significantly from all the previously described. They are geochemically evolved and enriched not only in Hf but also in rare metals Nb, Ta, W, Bi, and Sc, the non-formula elements Al, Ca, and Fe, and also in fluorine. Another remarkable feature is the strong vertical differentiation of zircon chemistry following vertical fractionation of parental granite within the 735 m deep section. Hf contents in zircon generally slightly increase upwards from 2–6 (median 3.3) wt% HfO_2 at the base of the zinnwaldite granite body at the depth of 550–735 m to 3–10 (median 7.0) wt% HfO_2 at the depth of 0–100 m; the Zr/Hf values decrease accordingly from 7–21 (median 12) to 3.3–12 (median 5.1). Mica-free granite and feldspathite at the depths of 284–369 m form a local positive deviation from this general trend reaching up to 12 wt% HfO_2 (Zr/Hf = 2.8), while partly sericitized granites at the depth of approximately 200 m contain zircon with less than 3.4 wt% HfO_2 (Zr/Hf = 9–16). Zircon from greisen bodies located in the uppermost part of the granite cupola differs from zircons from neighboring granites in its slightly lower Hf contents, mostly in the range of 2–5 (exceptionally up to 10, median 3.9) wt% HfO_2 and Zr/Hf = 4–11 (median 8).

Minor and trace element contents reach their maxima in zircon from the zinnwaldite granite: 1–5 wt% Y_2O_3, 1–3 wt% Yb_2O_3, 1.5–4 wt% UO_2, 1–3 wt% ThO_2, 1–3.5 wt% P_2O_5, 0.3–2.5 wt% Sc_2O_3, 0.5–1 wt% Nb_2O_5, around 1 wt% Bi_2O_3, etc. Referenced values represent common contents; occasionally substantially higher contents of all mentioned elements were found. Contents of up to 1 wt% Ta_2O_5, 4 wt% WO_3 or 1.5 wt% As_2O_5 were found in some grains, too.

Many zircon grains from zinnwaldite granites and greisens have been metamictized and altered. They display low analytical totals (occasionally down to 87 wt%) and contain 2–6 wt% of non-formula oxides of Al, Fe, Mn and Ca. The contents of fluorine in granitic zircon range within 0–2.5 (median 0.6) wt% F; in zircon from greisen, fluorine is ubiquitous, ranging 0.5–2.5 (median 0.7) wt% F. The contents of F generally increase with the decreasing analytical totals.

It should be mentioned that we found many zircon-like grains strongly enriched in P, As, Y, U and/or Th at Cínovec. These should be classified as transitional phases between zircon and xenotime, chernovite, coffinite and thorite (Förster 2006; Breiter et al. 2009; Förster et al. 2011). Such grains are usually relatively poor in Hf and are not discussed in this paper.

Whole-rock Zr and Hf contents

Whole-rock chemical compositions of granites from borehole CS-1, including Zr and Hf contents, have been published by Breiter et al. (in review). Major element and some trace element contents of volcanic rocks from borehole Mi-4 have been published and discussed in detail by Breiter (1997); high-quality Zr and Hf data were acquired for this paper. WR analyses of typical samples are shown in Table 5. Below, we comment only on recent Zr and Hf data obtained by ICP-MS (Fig. 6).

Within the calc-alkaline Schönfeld Unit, dacite displays slightly higher Zr and Hf contents (169–263 ppm and 4.6–7.4 ppm) than comagmatic rhyolite (105–119 ppm Zr, 3.4–3.7 ppm Hf); the Zr/Hf values increase from rhyolite to dacite from 30–32 to 36–39. A-type Teplice rhyolite contains 90–185 ppm Zr and 4.5–6.6 ppm Hf with relatively lower Zr/Hf values of 17–31. Inspecting the Mi-4 profile in more detail (Fig. 6a), the contents of Zr increase within each of the three eruptive units TR1–TR3 from the base to the top (93 → 149, 97 → 185, 123 → 146 ppm), while Hf contents are generally uniform. The Zr/Hf values thus increase within each eruption unit as follows: 21 → 29, 17 → 31, and 19 → 22.

Within the Cínovec granite cupola, the deeper seated biotite granite contains 120–150 ppm Zr and 6–8 ppm Hf with Zr/Hf

Table 4 Chemical composition of zircon as determined by EPMA analysis

Rock type	BR	BR	DC	DC	TR1	TR1	TR3	TR3	GP	BtG	BtG	ZiG
Locality borehole/depth	Mi-4/ 896	Mi-4/ 896	Mi-4 /608	Mi-4 /608	Mi-4 /578	Mi-4 /578	Mi-4 /50	Mi-4 /50	Loučná outcrop	CS-1 /1215	CS-1 /860	CS-1 /559
Sample No.	3219	3219	3211	3211	3210	3210	3194	3194	3531	4803	4802	4688
	Results of EPMA analyses (in wt%):											
SO_3	*bdl*	0.05	*bdl*	*bdl*	*bdl*	*bdl*	*bdl*	*bdl*	*bdl*	*bdl*	*bdl*	*bdl*
WO_3	*bdl*	*bdl*	*bdl*	*bdl*	*bdl*	*bdl*	*bdl*	*bdl*	*bdl*	*bdl*	*bdl*	0.67
P_2O_5	0.20	*bdl*	*bdl*	0.21	*bdl*	0.98	0.61	1.28	0.05	0.21	2.65	1.10
As_2O_5	0.06	*bdl*	*bdl*	0.22	*bdl*	0.05	*bdl*	0.12	*bdl*	*bdl*	0.47	1.30
Nb_2O_5	*bdl*	*bdl*	*bdl*	*bdl*	*bdl*	0.12	*bdl*	*bdl*	*bdl*	*bdl*	*bdl*	0.39
Ta_2O_5	*bdl*	*bdl*	*bdl*	*bdl*	*bdl*	*bdl*	*bdl*	*bdl*	*bdl*	*bdl*	*bdl*	*bdl*
SiO_2	30.94	31.01	32.15	28.72	31.71	25.40	29.55	21.40	31.99	29.65	25.88	24.76
TiO_2	*bdl*	*bdl*	*bdl*	*bdl*	*bdl*	0.09	*bdl*	0.22	*bdl*	*bdl*	*bdl*	*bdl*
ZrO_2	62.83	62.54	65.74	57.25	64.26	51.34	57.31	45.38	66.32	59.66	50.53	45.12
HfO_2	1.43	1.13	1.47	0.89	1.81	1.41	2.09	1.45	0.92	3.07	1.81	3.18
ThO_2	*bdl*	0.05	*bdl*	0.57	*bdl*	1.37	0.16	3.87	0.04	0.04	0.40	0.51
UO_2	0.34	0.06	0.07	0.83	0.14	1.21	2.06	1.17	*bdl*	0.85	1.08	1.35
Al_2O_3	*bdl*	*bdl*	*bdl*	1.09	*bdl*	0.81	*bdl*	0.76	*bdl*	0.20	0.38	0.75
Sc_2O_3	0.06	*bdl*	*bdl*	0.09	*bdl*	0.11	*bdl*	0.07	*bdl*	0.10	0.07	0.80
Y_2O_3	0.26	0.09	*bdl*	0.82	*bdl*	4.82	1.30	3.95	*bdl*	0.40	4.31	3.89
Ce_2O_3	*bdl*	*bdl*	*bdl*	*bdl*	*bdl*	*bdl*	*bdl*	0.42	*bdl*	*bdl*	*bdl*	0.52
Nd_2O_3	*bdl*	*bdl*	*bdl*	*bdl*	*bdl*	*bdl*	*bdl*	*bdl*	*bdl*	*bdl*	*bdl*	*bdl*
Sm_2O_3	*bdl*	*bdl*	*bdl*	*bdl*	*bdl*	0.10	*bdl*	*bdl*	*bdl*	*bdl*	*bdl*	*bdl*
Gd_2O_3	*bdl*	*bdl*	*bdl*	*bdl*	*bdl*	0.16	*bdl*	0.18	*bdl*	*bdl*	*bdl*	0.11
Dy_2O_3	*bdl*	*bdl*	*bdl*	0.11	*bdl*	0.80	0.26	0.69	*bdl*	*bdl*	0.45	0.89
Er_2O_3	*bdl*	*bdl*	*bdl*	0.11	*bdl*	0.68	0.27	0.54	*bdl*	0.15	0.71	0.92
Yb_2O_3	0.12	*bdl*	*bdl*	0.17	*bdl*	0.86	0.50	0.79	*bdl*	0.31	1.95	2.97
Bi_2O_3	0.10	*bdl*	0.10	*bdl*	*bdl*	*bdl*	*bdl*	*bdl*	0.10	*bdl*	*bdl*	0.93
MgO	*bdl*	*bdl*	*bdl*	*bdl*	*bdl*	*bdl*	*bdl*	*bdl*	*bdl*	*bdl*	0.06	*bdl*
CaO	*bdl*	*bdl*	*bdl*	0.89	*bdl*	1.73	1.84	2.58	*bdl*	0.29	0.84	1.93
MnO	*bdl*	*bdl*	*bdl*	0.14	*bdl*	0.06	0.65	0.58	*bdl*	*bdl*	0.25	0.80
FeO	0.06	0.07	0.06	1.93	0.08	1.20	0.34	6.04	0.12	0.19	1.40	1.13
PbO	*bdl*	*bdl*	*bdl*	*bdl*	*bdl*	*bdl*	0.11	*bdl*	*bdl*	*bdl*	*bdl*	*bdl*
F	*bdl*	*bdl*	*bdl*	0.23	*bdl*	0.63	0.42	0.46	*bdl*	0.12	0.51	0.66
Total	96.40	95.00	99.59	94.27	98.00	93.93	97.47	91.95	99.54	95.24	93.75	94.68
	Mineral formulae (in a.p.f.u.)*:											
S		0.001										
W												0.006
P	0.005			0.006		0.028	0.017	0.040	0.001	0.006	0.076	0.032
As	0.001			0.004		0.001		0.002			0.008	0.024
Nb						0.002						0.006
Ta												
Si	0.990	1.001	0.994	0.946	0.997	0.870	0.952	0.785	0.989	0.973	0.873	0.859
Ti						0.002		0.006				
Zr	0.980	0.984	0.991	0.920	0.985	0.857	0.900	0.812	0.999	0.954	0.831	0.763
Hf	0.013	0.010	0.013	0.008	0.016	0.014	0.019	0.015	0.008	0.029	0.017	0.031
Th		0.000		0.004		0.011	0.001	0.032	0.000	0.000	0.003	0.004
U	0.002	0.000	0.000	0.006	0.001	0.009	0.015	0.010		0.006	0.008	0.010

Table 4 (continued)

Rock type	BR	BR	DC	DC	TR1	TR1	TR3	TR3	GP	BtG	BtG	ZiG
Locality borehole/depth	Mi-4/ 896	Mi-4/ 896	Mi-4 /608	Mi-4 /608	Mi-4 /578	Mi-4 /578	Mi-4 /50	Mi-4 /50	Loučná outcrop	CS-1 /1215	CS-1 /860	CS-1 /559
Sample No.	3219	3219	3211	3211	3210	3210	3194	3194	3531	4803	4802	4688
Al				0.042		0.033		0.033		0.008	0.015	0.031
Sc	0.002			0.003		0.003		0.002		0.003	0.002	0.024
Y	0.004	0.002		0.014		0.088	0.022	0.077		0.007	0.077	0.072
Ce								0.006				0.007
Nd												
Sm						0.001						
Gd						0.002		0.002				0.001
Dy				0.001		0.009	0.003	0.008			0.005	0.010
Er				0.001		0.007	0.003	0.006		0.002	0.008	0.010
Yb	0.001			0.002		0.009	0.005	0.009		0.003	0.020	0.031
Bi	0.001		0.001						0.001			0.008
Mg											0.003	
Ca				0.031		0.063	0.064	0.101		0.010	0.030	0.072
Mn				0.004		0.002	0.018	0.018			0.007	0.024
Fe	0.002	0.002	0.002	0.053	0.002	0.034	0.009	0.185	0.003	0.005	0.039	0.033
Pb							0.001					
F				0.024		0.068	0.043	0.053		0.012	0.054	0.072
Zr/Hf wt.	75.3	94.6	76.4	109.4	60.8	62	46.9	53.4	123.7	33.2	47.7	24.2

Rock type	ZiG	MfG	FSP	ZiG	ZiG	greisen	greisen	greisen	greisen	Detection
Locality borehole/depth	CS-1 /559	CS-1 /308	CS-1 /305	CS-1 /24	CS-1 /24	CS-1 /53	CS-1 /53	South deposit	South deposit	limits
Sample No.	4688	4933	4932	4672	4672	CS-1 _10	CS-1 _10	South 6	South 10	
	Results of EPMA analyses (in wt%):									
SO_3	*bdl*	*bdl*	*bdl*	0.43	*bdl*	*bdl*	*bdl*	*bdl*	0.10	0.05
WO_3	0.25	*bdl*	*bdl*	0.50	*bdl*	4.23	1.02	*bdl*	2.72	0.10
P_2O_5	0.60	*bdl*	0.84	3.38	2.48	3.75	1.83	0.50	4.62	0.05
As_2O_5	0.90	1.03	0.62	0.78	0.76	0.59	1.46	0.50	0.45	0.05
Nb_2O_5	0.27	0.10	0.50	1.23	0.84	1.33	0.05	*bdl*	0.71	0.05
Ta_2O_5	*bdl*	*bdl*	*bdl*	0.32	*bdl*	0.06	*bdl*	*bdl*	*bdl*	0.05
SiO_2	27.15	26.80	25.12	23.11	23.26	14.71	20.45	26.19	11.84	0.05
TiO_2	*bdl*	*bdl*	*bdl*	*bdl*	*bdl*	*bdl*	*bdl*	*bdl*	*bdl*	0.05
ZrO_2	48.31	48.73	39.96	32.81	39.54	33.73	41.06	47.96	30.07	0.05
HfO_2	2.46	8.01	12.37	4.71	10.27	3.91	8.32	10.26	2.83	0.05
ThO_2	1.22	0.05	0.18	7.97	2.19	3.24	0.69	0.12	19.12	0.04
UO_2	1.03	1.03	2.61	2.53	3.46	2.09	1.15	1.10	0.87	0.04
Al_2O_3	3.85	1.16	0.99	0.74	0.60	0.15	0.77	0.55	0.51	0.05
Sc_2O_3	0.62	0.27	0.60	0.89	1.27	2.99	2.54	1.33	1.13	0.05
Y_2O_3	1.87	1.89	3.75	4.23	3.27	3.44	2.30	0.48	3.24	0.05
Ce_2O_3	0.58	0.18	0.36	0.29	0.20	0.11	0.15	*bdl*	0.20	0.08
Nd_2O_3	*bdl*	*bdl*	*bdl*	0.12	*bdl*	*bdl*	*bdl*	0.12	0.14	0.10
Sm_2O_3	*bdl*	*bdl*	*bdl*	0.14	0.11	0.16	0.11	*bdl*	0.17	0.10
Gd_2O_3	*bdl*	*bdl*	0.14	0.31	0.22	0.27	*bdl*	*bdl*	0.32	0.10

Table 4 (continued)

Rock type	ZiG	MfG	FSP	ZiG	ZiG	greisen	greisen	greisen	greisen	Detection
Locality borehole/depth	CS-1 /559	CS-1 /308	CS-1 /305	CS-1 /24	CS-1 /24	CS-1 /53	CS-1 /53	South deposit	South deposit	limits
Sample No.	4688	4933	4932	4672	4672	CS-1 _10	CS-1 _10	South 6	South 10	
Dy_2O_3	0.46	0.34	0.65	0.99	0.76	0.96	0.64	0.31	1.00	0.10
Er_2O_3	0.42	0.46	0.80	0.76	0.72	1.11	0.80	0.33	0.89	0.10
Yb_2O_3	1.80	1.17	1.80	1.63	1.47	2.84	2.13	0.89	1.99	0.10
Bi_2O_3	0.69	*bdl*	*bdl*	*bdl*	*bdl*	8.35	3.54	0.32	1.62	0.10
MgO	*bdl*	*bdl*	*bdl*	*bdl*	*bdl*	*bdl*	*bdl*	*bdl*	*bdl*	0.05
CaO	1.24	1.37	1.88	1.22	1.18	0.42	0.99	1.30	0.73	0.05
MnO	0.48	0.37	0.47	*bdl*	0.08	0.06	0.20	0.34	*bdl*	0.05
FeO	1.53	1.23	0.59	0.99	1.19	1.85	2.04	0.56	0.94	0.05
PbO	*bdl*	*bdl*	*bdl*	*bdl*	*bdl*	*bdl*	*bdl*	*bdl*	0.22	0.10
F	0.45	0.57	0.65	1.88	2.39	2.21	2.19	0.93	3.29	0.08
Total	96.18	94.76	94.88	91.96	96.26	92.56	94.43	94.09	89.72	
	Mineral formulae (in a.p.f.u.)*:									
S				0.011					0.003	
W	0.002			0.005		0.043	0.009		0.029	
P	0.017		0.025	0.102	0.071	0.124	0.055	0.015	0.161	
As	0.015	0.018	0.011	0.014	0.014	0.012	0.027	0.009	0.010	
Nb	0.004	0.002	0.008	0.020	0.013	0.024	0.001		0.013	
Ta				0.003		0.001				
Si	0.889	0.915	0.890	0.820	0.792	0.576	0.726	0.900	0.488	
Ti										
Zr	0.771	0.811	0.690	0.568	0.656	0.643	0.711	0.804	0.604	
Hf	0.023	0.078	0.125	0.048	0.100	0.044	0.084	0.101	0.033	
Th	0.009	0.000	0.001	0.064	0.017	0.029	0.006	0.001	0.179	
U	0.008	0.008	0.021	0.020	0.026	0.018	0.009	0.008	0.008	
Al	0.149	0.047	0.041	0.031	0.024	0.007	0.032	0.022	0.025	
Sc	0.018	0.008	0.019	0.028	0.038	0.102	0.079	0.040	0.041	
Y	0.033	0.034	0.071	0.080	0.059	0.072	0.043	0.009	0.071	
Ce	0.007	0.002	0.005	0.004	0.002	0.002	0.002		0.003	
Nd				0.002				0.001	0.002	
Sm				0.002	0.001	0.002	0.001		0.002	
Gd			0.002	0.004	0.002	0.004			0.004	
Dy	0.005	0.004	0.007	0.011	0.008	0.012	0.007	0.003	0.013	
Er	0.004	0.005	0.009	0.008	0.008	0.014	0.009	0.004	0.012	
Yb	0.018	0.012	0.019	0.018	0.015	0.034	0.023	0.009	0.025	
Bi	0.006					0.084	0.032	0.003	0.017	
Mg										
Ca	0.044	0.050	0.071	0.046	0.043	0.018	0.038	0.048	0.032	
Mn	0.013	0.011	0.014		0.002	0.002	0.006	0.010		
Fe	0.042	0.035	0.017	0.029	0.034	0.061	0.061	0.016	0.032	
Pb									0.002	
F	0.047	0.062	0.073	0.211	0.257	0.273	0.246	0.101	0.429	
Zr/Hf wt.	33.5	10.4	5.5	11.9	6.6	14.8	8.4	8	18.2	

Mineral formulae were calculated based on four oxygen atoms per formula unit; *bdl* Below the detection limit, *a.p.f.u.* Atoms per formula unit, *Zr/Hf wt.* Zr/Hf value by weight

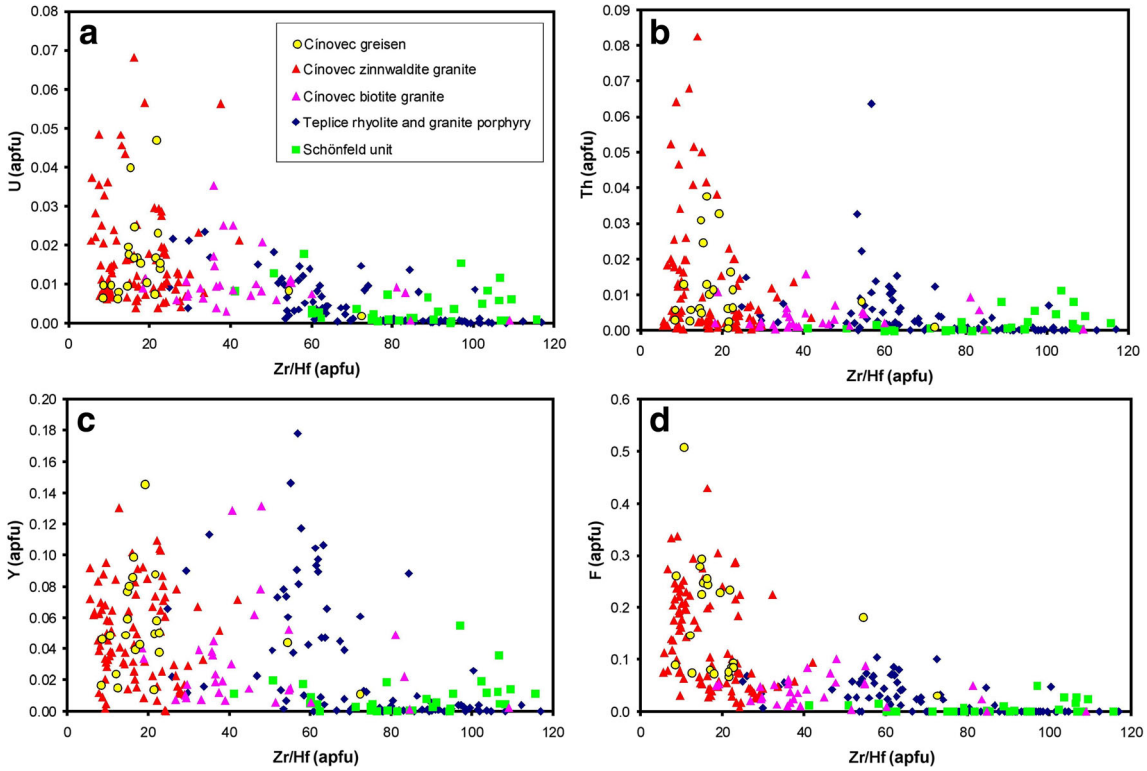

Fig. 4 Plots revealing ratios of chemical constituents in the zircon grains studied: **a**, Zr/Hf versus U; **b**, Zr/Hf versus Th; **c**, Zr/Hf versus Y; **d**, Zr/Hf versus F

values in the range of 18–22. Only a subtle general decrease upward (21 → 19) was encountered but local deviations of 24 and 13 were found. In contrast, the zinnwaldite granite shows a strong vertical differentiation: the early crystallized zinnwaldite microgranite (ZiGm) contains 80–120 ppm Zr; the later crystallized and vertically strongly fractionated zinnwaldite granite, however, shows an upwards decrease in Zr contants from approximately 80 ppm at depths of 600–735 m to approximately 40 near the actual surface. Because the contents of Hf vary insignificantly within the range of 5–8 ppm, Zr/Hf values mimic the Zr contents: they range between 12 and 14 in xenoliths of zinnwaldite microgranite and systematically decrease from 11 at the depth of 735 m to 8 at the depth of 100 m. In the uppermost part of the cupola, in the canopy, the Zr/Hf values equal approximately 4.5 (Fig. 6b). Worth mentioning is the fact that Zr/Hf values in greisens (6–7) equal those in the neighboring zinnwaldite granites (5–8).

Discussion

Zr/Hf values during differentiation of granitic melt

The Zr/Hf value is considered to be a reliable indicator of fractionation of granitic melt (Hanchar and Hoskin 2003; Claiborne et al. 2006; Zaraisky et al. 2009). We decided to test its functionality on the studied magmatic suites from the Teplice caldera (Fig. 7). To better understand the specific environment of A-type magmas, the following two typical peraluminous suites were added into figures: late orogenic peraluminous two-mica granites of the Moldanubian pluton, southern Czech Republic/Austria (Breiter 2016) and a rare-metal zinnwaldite granite from the Podlesí stock, Western Erzgebirge, Czech Republic (Breiter et al. 2005). A comparison of the Zr/Hf values with the most common indicator of fractionation, the K/Rb values (Fig. 7a), shows a good agreement in the general trend shifting from approximately K/Rb = 190 and Zr/Hf = 30–40 to K/Rb = 10 and Zr/Hf = 5–10. The scatter in the values of both ratios among individual samples of the biotite and zinnwaldite granites is caused by the different time of crystallization of major mineral hosts of K, Rb (K-feldspar, mica) and Zr, Hf (zircon), and probably also due to the inhomogeneous distribution of zircon in the rocks.

The correlation between the Zr/Hf and Nb/Ta ratios (Fig. 7b) is perfect in the A-type rocks from the caldera (Teplice rhyolite and all Cínovec granites) forming an array from ca. Nb/Ta = 13 and Zr/Hf = 30 to Nb/Ta = 1 and Zr/Hf = 5. We conclude that this perfect positive correlation strongly supports magmatic crystallization of major hosts of all mentioned elements, i.e., of zircon, rutile, columbite and Li-Fe micas. Peraluminous suites form an another, more widely scattered array with a relatively lower grade of Zr/Hf fractionation.

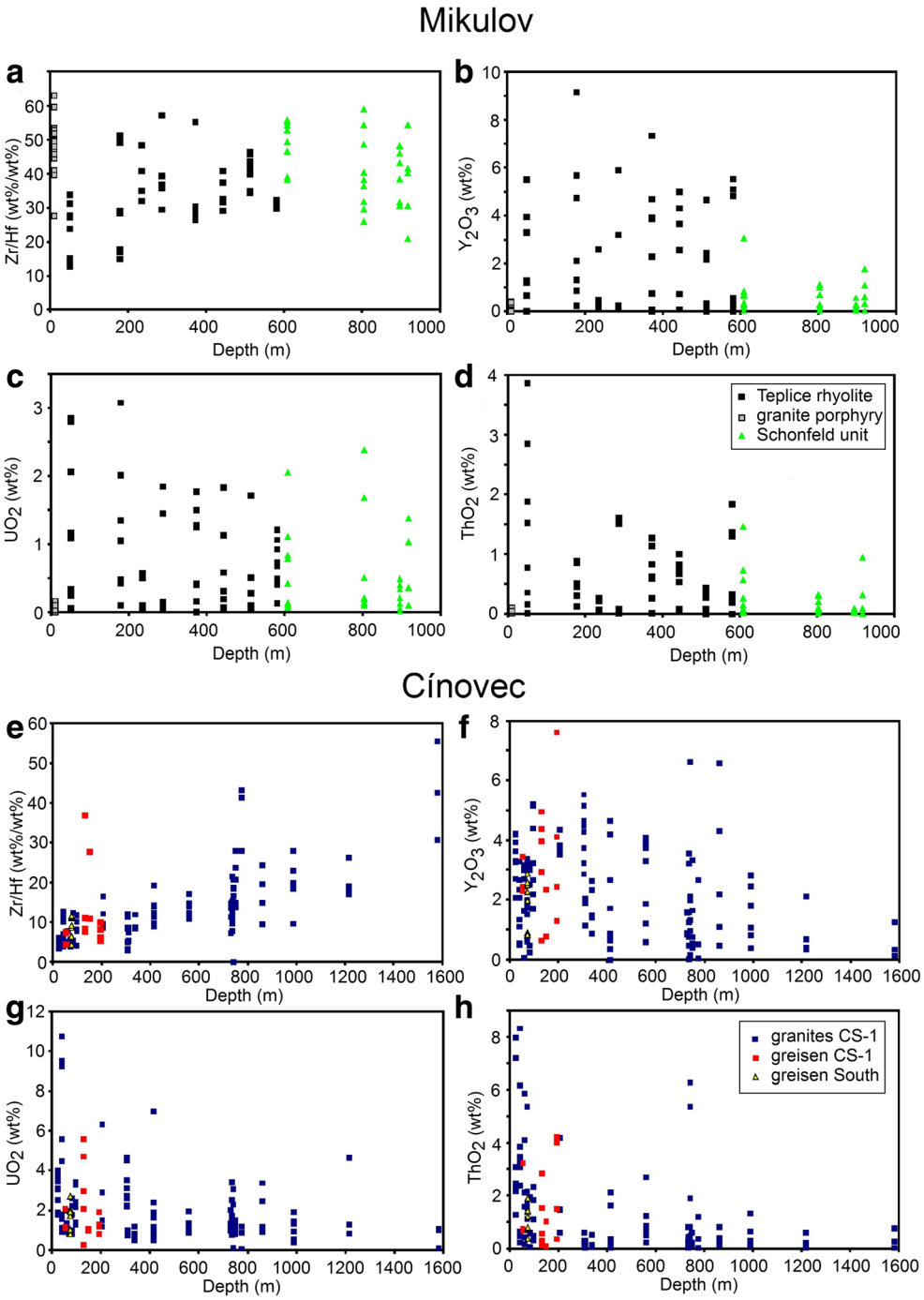

Fig. 5 Vertical zoning of the chemical composition of zircon in the two boreholes Mi-4 (**a**–**d**) and CS-1 (**e**–**h**)

A combination of the Zr/Hf ratio with the Rb/Sr ratio (Fig. 7c) shows a clear negative correlation; all suites form one array beginning at Rb/Sr = 0.5 and Zr/Hf = 35–40, and ending at Rb/Sr = 800 and Zr/Hf = 5–13. Small contents of Sr in zinnwaldite granites (often <10 ppm) can be easily affected by late magmatic to post-magmatic reactions with fluids. This explains the wide scatter of the values in the zinnwaldite granite samples.

Figure 8 illustrates in detail the behavior of Zr and Hf during fractionation of magmatic suites within the Teplice caldera in coordinates Hf vs. Zr and Hf vs. Zr/Hf. This figure also shows common peraluminous granites from the Moldanubicum and the Podlesí stock for comparison. Granites from the Moldanubian pluton show a linear trend with a perfect correlation between Zr and Hf (Zr 240 → 50 ppm, Hf 8 → 1.5 ppm, Fig. 8a) and a gradual decrease in the Zr/Hf value (Fig. 8b) from 35 to 24. Rare-metal granites

Table 5 Representative results of whole-rock analyses

Rock	BR	DC	TR1	TR1	GP	BtG	BtG	ZiG	ZiGm	MfG	FSP	greisen	ZiG
Locality borehole/depth	Mi-4/918	Mi-4/804	Mi-4/513	Mi-4/580	Loučná outcrop	CS-1 /1215	CS-1 /860	CS-1 /559	CS-1/ 413	CS-1/ 336	CS-1/ 305	CS-1/ 154	CS-1/ 60
Sample	3220	3216	3208	3210	3532	4803	4802	4688	4687	4686	4932	4930	4677
	Major constituents (in wt%):												
SiO_2	71.43	66.68	76.35	75.82	68.87	76.048	76.504	74.69	75.843	75.866	65.6	68.78	72.22
TiO_2	0.3	0.64	0.12	0.07	0.47	0.07	0.03	0.03	0.03	0.03	−0.01	−0.01	0.01
Al_2O_3	14.8	16.05	11.84	12.24	14.74	12.24	12.19	13.2	12.52	13.57	18.94	14.12	15.92
Fe_2O_3	0.41	0.63	1.02	0.37	1.59	0.66	0.67	0.32	0.45	0.43	0.3	0.97	0.20
FeO	1.14	2.32	0.35	0.43	1.81	0.63	0.91	0.58	0.72	0.05	0.1	3.48	0.45
MgO	0.76	1.54	0.14	0.08	0.065	0.1	0.07	0.03	0.02	0.06	0.25	0.01	0.09
MnO	0.040	0.108	0.031	0.020	0.450	0.041	0.057	0.057	0.077	0.021	0.024	0.329	0.086
CaO	1.11	2.09	0.45	0.8	1.62	0.69	0.49	0.35	0.39	0.38	0.53	0.44	0.38
Li_2O	0.006	0.011	0.002	0.002	0.005	0.047	0.053	0.167	0.115	0.004	0.005	0.87	0.216
Na_2O	2.23	3.04	1.18	2.41	3.64	2.89	3.09	4.02	3.96	4.02	3.84	0.08	4.83
K_2O	5.06	3.55	6.32	4.97	5.7	5.27	4.95	4.53	4.47	4.59	7.19	3.22	2.39
P_2O_5	0.092	0.254	0.017	0.011	0.147	0.012	0.011	0.012	0.014	0.01	0.023	0.02	0.015
F	0.063	0.038	0.042	0.445	0.085	0.467	0.471	0.752	0.655	0.154	0.333	4.724	0.792
L.O.I.	1.54	1.98	1.53	1.35	0.73	0.916	0.762	0.714	0.587	0.373	1.9	2.82	1.686
$H_2O(-)$	0.17	0.27	0.33	0.22	0.25	0.10	< 0.05	0.071	< 0.05	0.14	0.55	0.1	0.26
F(equ)	−0.027	−0.016	−0.018	−0.188	−0.036	−0.197	−0.199	−0.317	−0.276	−0.065	−0.141	−1.993	−0.334
Total	99.22	99.35	99.62	99.06	100.23	100.18	99.80	99.54	99.87	99.70	99.58	99.96	99.55
	Trace elements (in ppm):												
Ba	616	991	83	49	791	71	47	43	34	69	143	10	56
Be	5	1	3	5	4	16	11	11	14	7	8	16	9
Cs	19.6	12.5	11	8.3	14	26.5	27.5	34.5	32.1	10.5	29.7	133.5	31.7
Ga	18.2	19.2	17.1	20.2	22.6	24.3	27.8	39.8	31.8	41.3	55.7	38.5	53.9
Hf	3.7	5	5.2	4.5	10.2	8.5	9.1	6.8	8.7	4	8.9	8.7	9.1
Nb	10.6	12.6	9.7	16.9	16.3	51.4	60.8	74.3	67.7	81.9	46.8	76.2	109.3
Rb	256	154	248	399	208	772	948	1900	1390	1393	1956	3166	1441
Sn	9	18	3	11	6	95	9	23	84	7	1	36	127
Sr	220	449	22	26	136	13	10	5.8	8.6	10.2	8.5	4.5	72
Ta	1.2	1.4	0.8	1.8	1.1	7	11	31	17	30	25	31	52
Th	16.8	18.1	27.7	60	25	71	57	32	43	12.2	4.9	15	15
U	10.4	8.1	5.6	16	6.1	45	32	8.6	46	6.5	42	10.4	4
W	3.8	3.9	2.2	1.5	0.9	13.6	16.5	41.2	26.9	5.3	3.5	473.2	13.3
Zr	119	197	149	93	380	147	138	58	106	31.3	62	52	44
Y	19.7	17	21.6	44	38	123	146	49	131	21.1	18.2	11.3	7.5
La	29.3	45.2	54.9	33.1	69.7	36.2	36.6	22.5	30.5	13.1	4.2	7	3.9
Ce	57.2	86.9	116	79.4	140	84.8	93.8	62.2	79.9	43.8	9.8	19.7	13.5
Pr	6.37	9.57	13.27	10.02	15.49	10.55	11.56	7.2	10.18	4.88	1.08	2.22	1.84
Nd	22.1	34	46.9	40.2	58.8	39.8	43.2	21.7	36.2	13.6	3	5.8	4.9
Sm	4.04	5.78	7.43	9.5	9.58	11.69	13.03	6.43	11.15	3.82	1.05	1.75	1.54
Eu	0.62	1.24	0.12	0.07	1.22	0.12	0.04	<0.02	<0.02	<0.02	0.02	<0.02	<0.02
Gd	3.68	4.56	5.17	8.04	7.93	12.29	13.57	5.4	11.15	2.91	1.2	1.37	1.03
Tb	0.54	0.57	0.78	1.34	1.23	2.71	3.13	1.39	2.76	0.79	0.4	0.4	0.33
Dy	3.14	3.15	4.28	7.63	6.73	19.26	21.72	10.07	19.31	5.35	3.59	3	2.41

Table 5 (continued)

Rock	BR	DC	TR1	TR1	GP	BtG	BtG	ZiG	ZiGm	MfG	FSP	greisen	ZiG
Locality borehole/depth	Mi-4/918	Mi-4/804	Mi-4/513	Mi-4/580	Loučná outcrop	CS-1 /1215	CS-1 /860	CS-1 /559	CS-1/ 413	CS-1/ 336	CS-1/ 305	CS-1/ 154	CS-1/ 60
Sample	3220	3216	3208	3210	3532	4803	4802	4688	4687	4686	4932	4930	4677
Ho	0.66	0.56	0.8	1.41	1.24	4.16	4.83	2.11	4.38	1.06	0.89	0.68	0.51
Er	1.89	1.53	2.25	4.17	3.59	13.16	16.42	7.21	14.91	3.69	3.85	2.36	1.9
Tm	0.27	0.22	0.35	0.62	0.55	2.25	2.83	1.56	2.76	0.77	0.82	0.57	0.46
Yb	1.8	1.52	2.4	4.24	3.38	15.88	20.05	12.4	20.77	6.3	7.07	5.1	4.22
Lu	0.25	0.23	0.36	0.58	0.5	2.33	3.14	1.88	3.1	0.95	1.15	0.81	0.65

L.O.I. = loss on ignition; $H_2O(-)$ = loss of moisture by heating up to 105 °C; F(equ) = correction for the oxygen equivalent of F

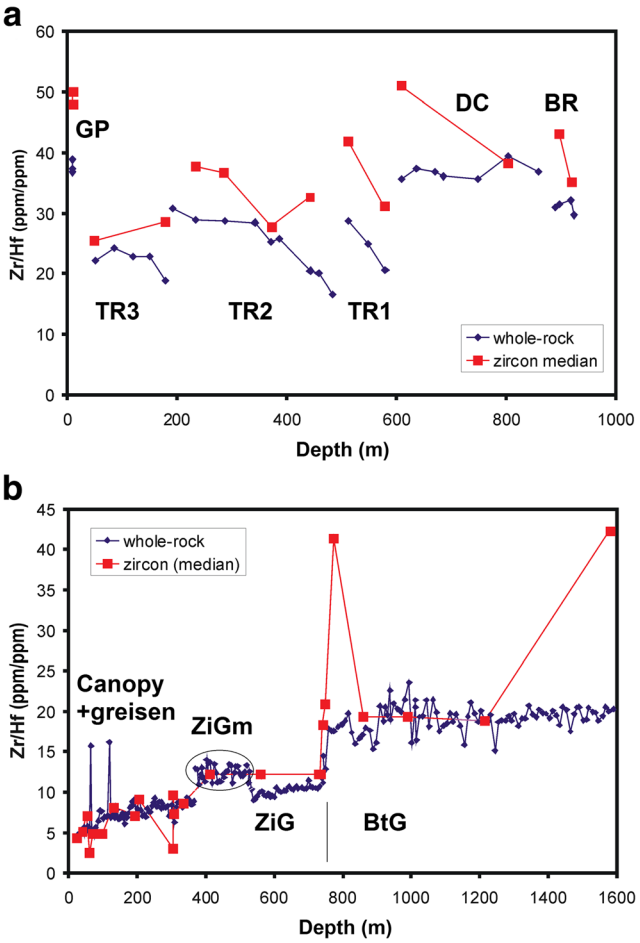

Fig. 6 A comparison of Zr/Hf values in zircon grains (medians) and parental rocks along the two boreholes studied: **a**, Mi-4; **b**, CS-1. Data from granite porphyry are shown for comparison

from the Podlesí stock are generally poor in Hf (1.5–3 ppm), and the decrease in the Zr/Hf values (23 → 9) is largely controlled by the decrease in Zr (50 → 17 ppm Zr). The peraluminous Schönfeld Unit from the Teplice caldera shows a Zr and Hf evolution similar to that in the Moldanubian granites: the decrease in both Zr (184–263 to 105–119 ppm) and Hf (4.6–7.4 to 3.4–3.7 ppm) contents from dacite to basal rhyolite is accompanied by a decrease in the Zr/Hf values from 36–39 to 30–32. Consequently, the moderately fractionated peraluminous suites (Schönfeld volcanic and Moldanubian two-mica granites) evolved via a regular decrease in both Zr and Hf, accompanied by a moderate decrease in the Zr/Hf values. The Podlesí stock of zinnwaldite granite represents water-rich residual melt influenced by explosive degassing and undercooling (Breiter et al. 2005) with a rather chaotic distribution of Zr, Hf and other HFSE (Breiter et al. 2006).

The behavior of Zr and Hf in the Cínovec A-type granites is quite different: Both patterns show a considerable scatter in the Hf contents in both granites and greisens, which did not change during the entire evolution of the pluton, remaining in

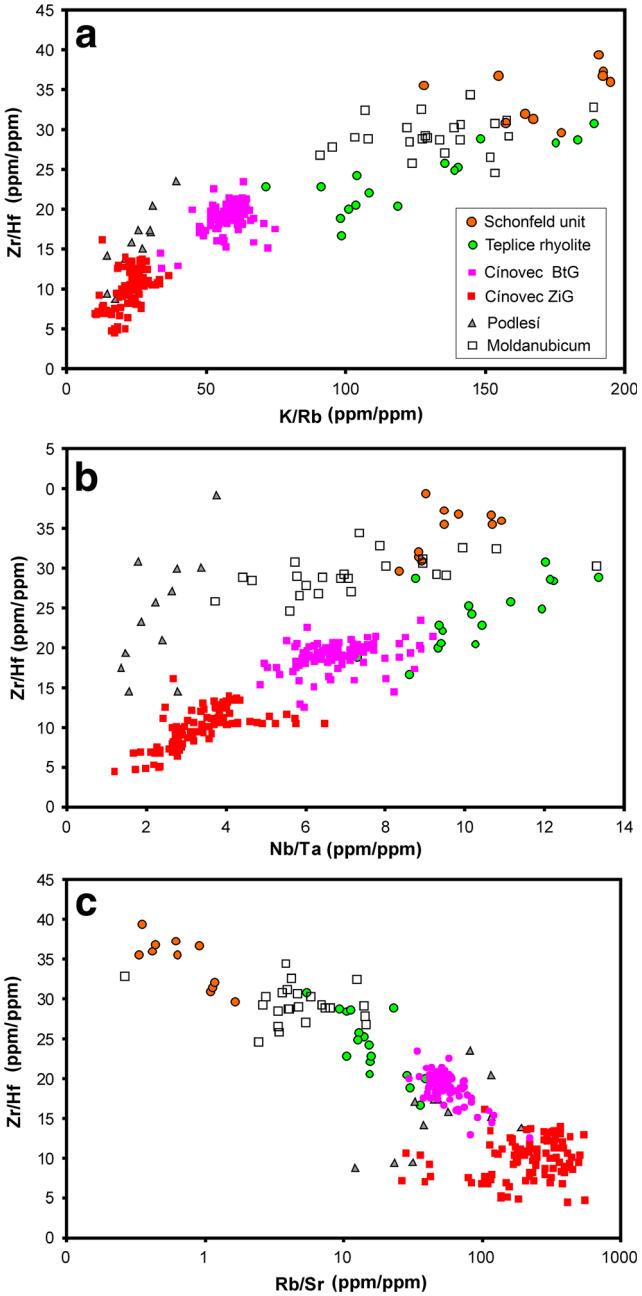

Fig. 7 A comparison of whole-rock Zr/Hf values with that of other common indicators of magma fractionation: **a**, Zr/Hf versus K/Rb; **b**, Zr/Hf versus Nb/Ta; **c**, Zr/Hf versus Rb/Sr. Comparative data from the Moldanubian two-mica granites and zinnwaldite granites from the Podlesí stock are present authors unpublished data

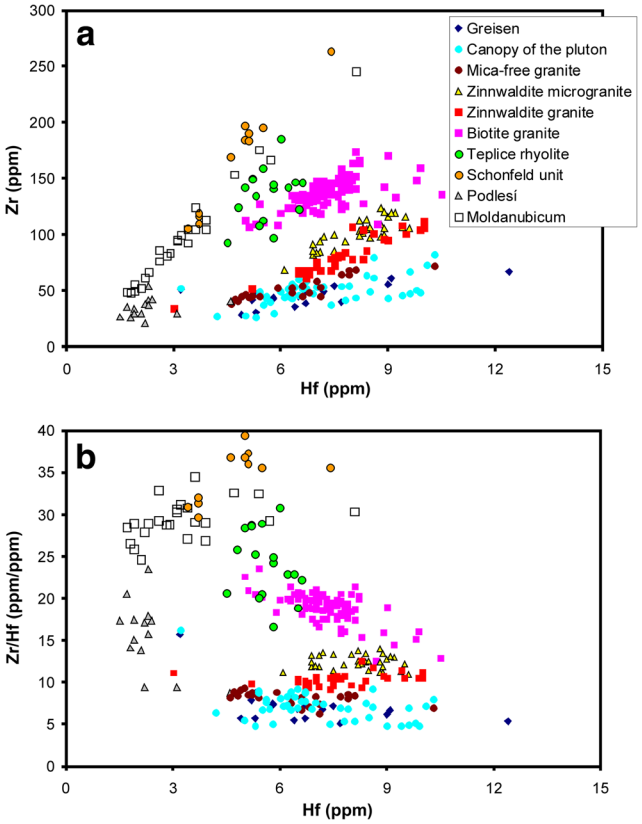

Fig. 8 Whole-rock evolution of Zr and Hf contents and the Zr/Hf ratio: **a**, Zr plotted against Hf; **b**, Zr/Hf plotted against Hf. Data for the Moldanubian and Podlesí plutons are from Breiter (2016) and Breiter et al. (2005)

the range of 4.5–10.5 ppm Hf (medians 7–8 ppm Hf for all rock types). The decrease in the Zr/Hf values from approximately 22 to 5 is controlled almost exclusively by a depletion in Zr from 170 to 25 ppm. Within each rock type we found a good positive correlation between Zr and Hf (Fig. 8a), which is caused by the varying amount of zircon grains in the individual samples, i.e., m-size inhomogeneity of the zircon distribution in granite.

In the A-type Teplice rhyolite, Zr and Hf contents in the individual samples scattered but the general decrease in Zr/Hf values correlated well with volcanic stratigraphy (Breiter et al. 2001) and other indicators of magmatic fractionation (Fig. 7).

Zr/Hf values of zircon grains and their host rocks

The behavior of likely no other chemical element is linked with a single mineral as is the behavior of zirconium and hafnium linked with mineral zircon. This leads to a simple interpretation that the relationship between Zr and Hf found in zircon is applicable to the behavior of Zr and Hf in granite (magma) and vice versa (Butler and Thompson 1965). Zr and Hf may theoretically be fractionated by amphibole, clinopyroxene, garnet and titanite but the low contents of these minerals and low KD values minimized their real influence (Claiborne et al. 2006). Nevertheless, a detailed analysis of large data sets shows that the relationship between the Hf content (Zr/Hf ratio) in zircon and its parent rock is not straightforward.

Figure 9 shows that most of the analyzed zircon grains from the relatively less fractionated rocks (Schönfeld Unit, Teplice rhyolite and Cínovec biotite granite) yielded higher

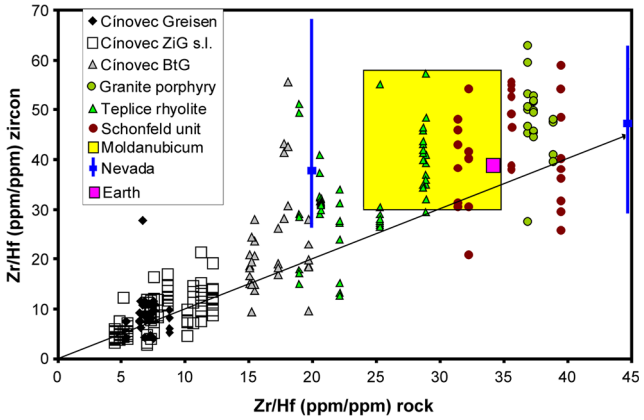

Fig. 9 Deviation of Zr/Hf values in zircon from Zr/Hf values in the parental melt. Data for the mean of granitic zircon on the Earth are combined from Wang et al. (2010) and Patzer et al. (2010), data for the Moldanubian pluton are from Breiter (2016). Data from the Spirit Mountain batholith, Nevada (whole scatter of individual zircon analyses and their medians from monzonite and leucogranite) come from Claiborne et al. (2006). The ideal correlation Zr/Hf_{zircon} versus $Zr/Hf_{WR} = 1$ Black line) is shown as visual guide

Zr/Hf values than the parent magmatic rock. Only in the case of the Cínovec zinnwaldite granite and its derivatives (greisens) the means of zircon Zr/Hf values approximately equal the host rock values. In this figure, average values for the granitoid zircon on the Earth (Wang et al. 2010), the area occupied by zircons from common latecollisional peraluminous two-mica granites from the Moldanubicum, Bohemian Massif (Breiter 2016), and for two successive granitoids (monzonite, leucogranite) from the Spirit Mountain batholith, Nevada (Claiborne et al. 2006) are also shown for comparison. The Earth average of granitic zircon and a great majority of zircon grains from the Moldanubicum also display higher Zr/Hf values than the corresponding parent rocks, similar to zircon from the Teplice caldera with an analogous grade of host rock fractionation. Interesting is the evolution of the Spirit Mountain batholith: both analyzed samples show a large dispersion of Zr/Hf values in zircon, but the median of Zr/Hf values from the less fractionated monzonite nearly equals that of the whole-rock values (47 in zircon vs. 45 in the rock). In contrast, all zircon analyses from the more fractionated leucogranite give much higher Zr/Hf values (25–68, median 38) than the whole rock value 20.5 (Claiborne et al. 2006).

Granitoids do not contain any other real host of Zr and Hf besides zircon. Therefore, average Zr/Hf values in zircon should equal average Zr/Hf values in the whole rock. A possible explanation for the discrepancy shown in Fig. 9 is the presence of thin Hf-enriched rims on zircon crystals. Even a thin rim can be volumetrically significant (e.g., 3 μm rim of a 50 μm cubic core represents 29 vol.% of the grain). This model is, however, not consistent with the detailed measurements by Claiborne et al. (2006): the relatively Hf-enriched zircon rims still showed Zr/Hf values higher than those of the host leucogranite. An another, probably a more realistic, explanation is the existence of a population of very small, late-crystallized Hf-enriched zircon grains. These may be overlooked or, if found, they may not get analyzed due to their small sizes.

Strongly fractionated rocks, here represented by zinnwaldite granites, are Zr-poor, and the zircon saturation occurred locally at the very end of the crystallization of the melt; most zircon grains crystallized in interstices. These grains are small (approximately 20 μm) and not zoned; therefore, their analyses better match the whole-rock composition.

A strong negative effect of peraluminity on zircon and hafnon solubility was experimentally established by Linnen and Keppler (2002). Consequently, Zaraisky et al. (2009) explained experimentally the decrease in the Zr/Hf values during pronounced fractionation of F-enriched rare-metal and pegmatite melts. At 800 °C, 1 kbar, ASI = 1.2 and F content between 1 and 2 wt%, which is well comparable with the condition in the carapace of the Cínovec pluton, they found $Zr/Hf_{zircon} \sim 6$, while $Zr/Hf_{melt} \sim 4.3$. This perfectly coincides with the most fractionated samples of granite from the top of the Cínovec cupola and their zircon (Fig. 9).

Zr/Hf fractionation, a key to correct interpretation of magmatic suite evolution

Variations in whole-rock Zr/Hf values along boreholes Mi-4 and CS-1 in combination with medians of Zr/Hf values in zircon are shown in Fig. 6. This figure can be analyzed from the following two perspectives: (i) conformity of both variables, i.e., similarity of the whole-rock and zircon Zr/Hf values, and (ii) continuous or discontinuous evolution of the Zr/Hf patterns, i.e., general geochemical evolution of the suites. In both cases, the two discussed boreholes provide contrasting examples.

Ad (i): At Cínovec (Fig. 6b), a good agreement is observed between the Zr/Hf values in zircon and the whole rock. Anomalously high values were encountered only in zircon grains from two samples of biotite granite. The shape of these zircon grains does not differ from that from other samples with "correct" Zr/Hf values; these samples perhaps reflect an accumulation of early zircon grains crystallized at the beginning of magma solidification. In contrast, almost all zircon grains from the Teplice rhyolite (Fig. 6a) exhibit much higher Zr/Hf values than the whole rock. In this case, larger zircon grains, grown up early in a deep magma reservoir, were probably analyzed. A part of Zr and Hf, still dissolved in the melt at the time of the eruption, were then incorporated into rapidly crystallizing microzircons (<1 μm) or remained dispersed in volcanic glass. The observed differences are consistent with the hypothesis of Erdmann et al. (2013) that zircon grains with

higher Zr/Hf values grow from early water-unsaturated melts, while the late zircon grains with low Zr/Hf values crystallized from water-saturated residual melts. This may also explain the origin of some extremely Hf-enriched zircon grains at the top of the granite cupola.

Ad (ii): a large number of whole-rock samples from borehole CS-1 at Cínovec (Fig. 6b) sensitively indicates several petrologic boundaries, in particular at depths of 735 m, 522 m and 368 m. Biotite granite is richer in Zr and displays higher Zr/Hf values and a wider local Zr/Hf variability but exhibits no systematic vertical variation; all textural varieties of biotite granite contain zircons of identical chemical compositions. In contrast, zinnwaldite granite shows a distinct vertical Zr/Hf development but it is much less variable in detail than the biotite granite. Upward fractionation of the zinnwaldite granite reduced the Zr/Hf value from 10–11 at a depth of approximately 700 m to approximately 5 in the uppermost 100 m of the borehole. Higher Zr/Hf values at a depth of ca 380–500 m correspond to rafts of zinnwaldite microgranite, which represent the first portion of the solidified melt along the upper contact of the intrusion. This "carapace granite" (sensu Cobbing et al. 1986) was later broken and plunged down into viscous melt (Breiter et al. in rev). Vertical variation in Zr/Hf is in perfect accordance with upwards enrichment in lithophile and ore elements (Li, Rb, Nb, Ta and F, Breiter in rev.).

Despite of the significantly lower number of samples analyzed from borehole Mi-4, independent vertical/temporal evolution of all three eruption units of the Teplice rhyolite is well constrained (Fig. 6a). The Teplice rhyolite evolved as three subsequent comagmatic magma batches. Each eruption started with geochemically more evolved material (low Zr/Hf) from the top of the reservoir and terminated with cumulate-enriched, geochemically primitive magma portion (high Zr/Hf) from the bottom of the reservoir.

Influence of magmatic fluids on Zr/Hf ratios

London et al. (1988) found experimentally that $D^{fluid/melt}$ for Hf is higher than that for Zr at conditions relevant to rare-metal granites and pegmatites; they concluded that hydrothermal zircon may be Hf-enriched. Crystallization of Hf-rich zircon rims in A-type rare-metal granites from Na, F-rich fluids during albitization was proposed by Kempe et al. (2004). Particularly at Cínovec, the origin of Hf-rich zircon via metasomatic fluorination was explained by Johan and Johan (2005).

Recent detailed studies of natural systems provided the following different results: while hydrothermal rims on zircon from the Koktokay pegmatite, China, are extremely Hf-enriched (Yin et al. 2013), hydrothermal zircon from Tanco pegmatite, Canada, is Hf-impoverished compared to the foregoing magmatic zircon population (Van Lichtervelde et al. 2009). At Cínovec, an 85 m thick zone of mica-free granite with feldspathite intercalations appears at a depth of 284–369 m in borehole CS-1, i.e., approximately 100 m below the major greisen bodies. Mica-free granite is supposed to be a restite after exsolution of a F, Li, Sn-rich fluid which induced greisenization in the uppermost part of the granite cupola (Breiter et al. in rev). This rock contains zircon with 4–12 wt% HfO_2 and Zr/Hf = 3–8, i.e., with a similar or slightly higher Hf content and lower Zr/Hf value than neighboring granites. Greisen bodies located within the uppermost 200 m of the borehole exhibit identical Zr/Hf whole-rock values and contain zircon with a chemical composition similar to that of the surrounding granites.

The strong enrichment in Nb (up to 4 wt% Nb_2O_5) and Ta (up to 1 wt% Ta_2O_5) in zircon from Cínovec, much higher than generally reported from zircon (Belousova et al. 2002, Nardi et al. 2013, Grimes et al. 2015), may arise suspicion of strong hydrothermal alteration, i.e., secondary enrichment in Nb, Ta, and potentially other HFSE including Hf. Nevertheless, Van Lichtervelde et al. (2009) found up to 4.7 wt% Ta_2O_5 in a U, Th-poor, i.e., non-metamict zircon from the Tanco pegmatite and then synthesized zircon with up to 3.7 wt% Ta_2O_5 in laboratory conditions (Van Lichtervelde et al. 2011). We conclude that the Nb, Ta-rich zircon grains need not have necessarily undergone a strong reaction with fluids and, as such, they retain primary Zr/Hf values. Altogether, no evidence of fluid-related enhancement of Hf has been found.

Possible influence of late fluids on Zr/Hf values in zircon

Zircon grains in the studied granites are usually enriched in radioactive elements U (mostly approximately 1 wt%, occasionally >4 wt% UO_2) and Th (often 1–5 wt% ThO_2). Some of them exhibit patchy zoning, an enrichment in the non-formula elements Al, Ca, Fe, Mn and Mg, and their analytical totals are reduced to 90–95 wt%. Low analytical totals down to 90 wt% and the uptake of water and non-formula elements into zircon are explained by an alteration of a previously radiation-damaged (i.e. metamictized) material in a fluid-driven reaction (Nasdala et al. 2009). Metamictization and related fluid-driven alteration affected mainly the cores of the studied grains (see typical examples in Fig. 3a, g), which are enriched in U and/or Th, while the rims are sometimes slightly enriched in Hf. Relatively low Hf in the core can be explained via crystallization from the initial melt poor in Hf, or via selective dissolution of Hf after metamictization. Zircon from the Teplice rhyolite is relatively poor in U and Th but also often exhibits features typical for metamict zircon.

We tried to resolve whether a reaction of metamictized zircon with aqueous fluid may alter the Zr/Hf value. Anderson et al. (2008) found the amorphous domain in natural metamict zircon to be relatively enriched in Hf compared to

the associated highly crystalline zircon; the primary magmatic or late post-metamict origin of this enrichment could not be determined. The Zr/Hf value in a 619 Ma old zircon from the Eastern Desert, Egypt remained unaffected up to an alpha dose of 13.7 × 10^{18} events/g but strongly fluctuated above 20 × 10^{18} α-events/g (Geisler et al. 2003b).

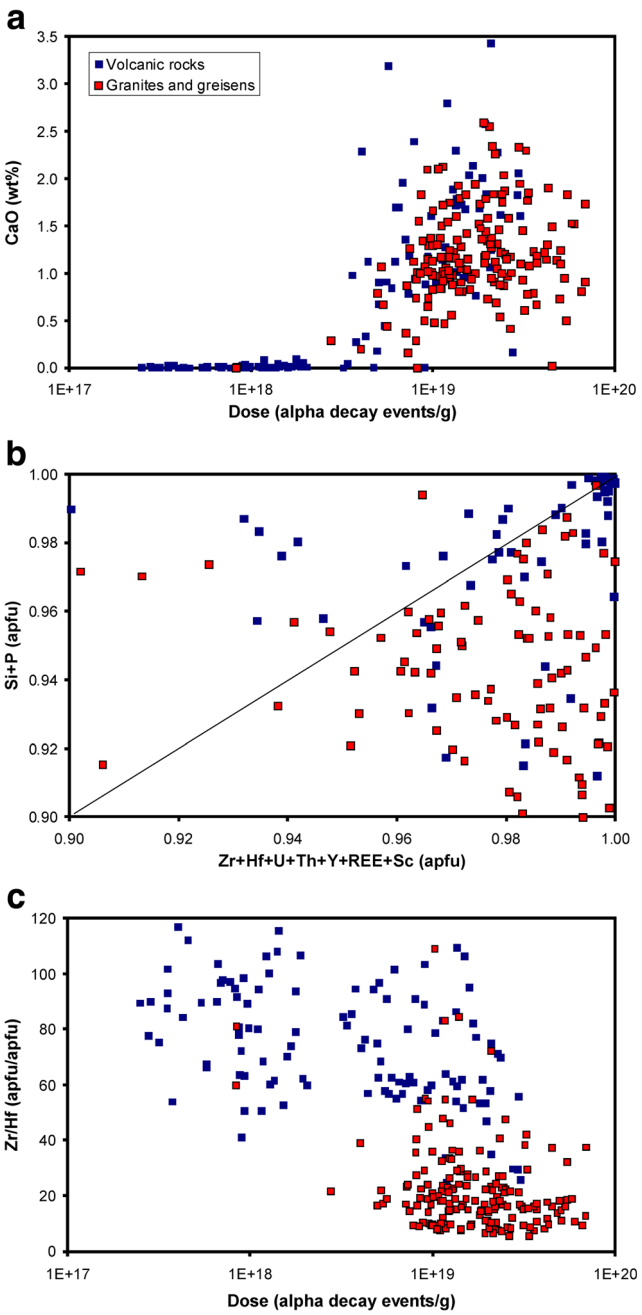

Fig. 10 Influence of radiation-induced damage (expressed using the alpha dose calculated for a model age of 320 Ma) and subsequent alteration on the chemical composition of zircon: **a**, The relation of CaO content and alpha dose shows that only zircon with a cumulative dose exceeding 3 × 10^{18} α/g incorporates non-formula elements like Ca (Al, Fe, Mn, Mg); **b**, the relation of Si + P (B-site elements) and Zr + Hf + U + Th + Y + REE + Sc (A-site elements) shows that the B-site elements (mainly Si) are more easily released from the zircon lattice than the A-site elements (mainly Zr and Hf); **c**, the plot of Zr/Hf against alpha dose indicates that these two parameters are not correlated. Not that in **b**, only elements were considered that are reliably bound in the zircon crystal lattice

According to the experiments, the Zr/Hf values are generally stable in contact with hot (350–650 °C) $CaCl_2$- and $AlCl_3$-bearing fluids (Geisler et al. 2003a) but a small decrease from 58 to 51 was observed at 175 °C and 1 M HCl-$CaCl_2$ fluid (Geisler et al. 2002). According to Geisler et al. (2003a) and Schmidt et al. (2006), Zr migrates at only very short distances within a single grain after the dissolution of radiation-damaged domains of zircon, being incorporated into recrystallized matter again. Wood (2005) and Linnen and Cuney (2005) agreed that the solubility of Hf in aqueous fluids is higher than that of Zr but no experimental evidence for natural zircon is available. Altogether, it can be only speculated that a relative Hf impoverishment in metamictized zircon cores may be partly caused by selective dissolution in fluid.

According to Ewing et al. (2000), zircon from the Variscan granites (model age 320 Ma) will be actually metamict if it contains more than 0.4 wt% U (0.45 wt% UO_2); about 75% of analyzed zircon grains from the Teplice caldera exceed this limit in their U contents, and 13% of analyzed grains exceed 3 wt% UO_2. So, the major part of the studied zircon grains should be considered metamict. The content of 0.4 wt% U in 320 Ma old zircon corresponds to a cumulative alpha dose of ~4 × 10^{18} events/g. As shown in Fig. 10a, substantial contents of non-formula elements are characteristic for zircon grains with an alpha dose of >3 × 10^{18} α/g, which is in good agreement with the estimate of Ewing et al. (2000). At the same alpha dose, the analytical totals drop to 95–90 wt%. Figure 10b illustrates that the B-site elements (Si accompanied by P as a part of the isostructural "xenotime component") are released more easily than the A-site elements; this indicates a relatively low mobility of Zr and Hf in damaged zircon. Approximately one fifth of the zircon grains analyzed have experienced an alpha dose exceeding 2 × 10^{19} α/g, which represents the threshold for possible Zr/Hf decoupling (Geisler et al. 2003b). Nevertheless, Fig. 10c indicates that the low Zr/Hf values in zircon from Cínovec granites are not correlated with the alpha dose. Thus, the low Zr/Hf values were not noticeably changed after metamictization.

Conclusions

A detailed study of Hf contents and Zr/Hf ratios in zircon and its parental rock from the Teplice caldera led to the following generalized conclusions:

- Zr/Hf values in the whole rock may serve as a sensitive indicator of the fractionation of evolved granitic melts (rhyolites, granites, pegmatites), only very weakly influenced by secondary fluid-related processes.

- Zr/Hf values in individual zircon grains are scattered but their general evolution trend in a rock series is consistent with the evolution of the whole-rock Zr/Hf values.
- Whole-rock contents of both Zr and Hf during the differentiation of S-type magma equally decrease, being accompanied by a moderate decrease in the Zr/Hf values. In the A-type suites, however, Hf contents remain nearly constant, and a strong decrease in the Zr/Hf values is controlled only by a decrease in Zr contents.
- Mica-free granite facies at Cínovec, produced after the exsolution of F, Li-rich late magmatic fluids, contain zircon with very low Zr/Hf values; there is no evidence of preferred partitioning of Hf into fluids.
- Quartz-zinnwaldite greisens show the same Zr/Hf whole-rock values and contain zircon identical with that in the neighboring granites in its chemical composition. There is no indication of an influence of F, Li-rich fluids on zircon during greisenization.
- Actual results support the hypothesis by Erdmann et al. (2013) that zircon crystallizing from a water-unsaturated melt is Hf-depleted, while zircon crystallizing from a water-saturated melt is identical with the parental melt in its Zr/Hf values or is relatively Hf-enriched compared to the parental melt.
- The most fractionated samples from the canopy of the A-type Cínovec pluton fit well the experiments by Zaraisky et al. (2009) for a slightly peraluminous, F-rich melt having Zr/Hf ~4.5–5.5 and containing zircon with Zr/Hf median of ~4.5–5.0.

Acknowledgements Constructive comments and suggestions of four anonymous experts and the Editor-in-Chief L. Nasdala are gratefully acknowledged. This work was supported by the Czech Science Foundation, project number GA 14-13600S to the Institute of Geology, Czech Academy of Sciences, and to the Faculty of Science, Masaryk University.

References

Ackerman L, Haluzová E., Creaser RA, Pašava J, Veselovský F, Breiter K, Erban V, Drábek M (2016) Re-os geochronology of molybdenites from the Bohemian Massif with the implications for the timing of mineralizations. Mineral Deposita (in press; doi:10.1007/s00126-016-0685-5)

Anderson AJ, Wirth R, Thomas R (2008) The alteration of metamict zircon and its role in the remobilization of high-field-strenght elements in the Georgeville granite, Nova Scotia. Can Mineral 46:1–18

Belousova EA, Griffin WL, Oreilly SY, Fisher NI (2002) Igneous zircon: trace element composition as an indicator of source rock type. Contrib Mineral Petrol 143:602–622

Breiter K (1997) Teplice rhyolite (Krušné hory Mts., Czech Republic) chemical evidence of a multiply exhausted stratified magma chamber. Věstník Českého geologického Ústavu 72:205–213

Breiter K (2012) Nearly contemporaneous evolution of the A- and S-type fractionated granites in the Krušné hory/Erzgebirge Mts., Central Europe. Lithos 151:105–121

Breiter K (2016) Monazite and zircon as major carriers of Th, U, and Y in peraluminous granites: examples from the Bohemian Massif. Mineral Petrol 110:767–785

Breiter K, Čopjaková R, Škoda R (2009) The involvement of F, CO_2-, and as in the alteration of Zr-Th-REE-bearing accessory minerals in the Hora Svaté Kateřiny A-type granite, Czech Republic. Can Mineral 47:1375–1398

Breiter K, Förster H-J, Škoda R (2006) Extreme P-, Bi-, Nb-, Sc-, U- and F-rich zircon from fractionated perphosphorus granites: the peraluminous Podlesí granite system, Czech Republic. Lithos 88:15–34

Breiter K, Lamarao CN, Borges RMK, Dallagnol R (2014) Chemical characteristic of zircon from A-type granites and comparison to zircon of S-type granites. Lithos 192-195:208–225

Breiter K, Müller A, Leichmann J, Gabašová A (2005) Textural and chemical evolution of fractionated granitic sytem: the Podlesí stock, Czech Republic. Lithos 80:323–345

Breiter K, Müller A, Shail R, Simons B (2016) Chemical composition of zircons from the Cornubian Batholith of SW England and comparison with zircons from other European Variscan rare-metal granites. Mineral Mag 80:1273–1289

Breiter K, Novák J, Chlupáčová M (2001) Chemical evolution of volcanic rocks in the Altenberg-Teplice caldera (Eastern Krušné Hory Mts., Czech Republic, Germany). Andean Geol 13:17–22

Breiter K, Škoda R (2009) Accessory minerals of ABO_4-type from some subvolcanic equivalents of A-type granites from the Krušné hory/Erzgebirge Mts. and from the Teplice rhyolite. Geosci Res Rep for 2008:147–151

Breiter K, Škoda R (2012) Vertical zonality of fractionated granite plutons reflected in zircon chemistry: the Cínovec A-type versus the Beauvoir S-type suite. Geol Carpath 63:383–398

Broska I, Bibikova E, Gracheva T, Makarov V, Cano F (1990) Zircon from granitoid rocks of the Tríbeč-Zobor crystalline complex; its typology, chemical and isotopic composition. Geol Carpath 41:393–406

Butler JR, Thompson AJ (1965) Zirconium: hafnium ratios in some igneous rocks. Geochim Cosmochim Ac 29:167–175

Cháb J, Breiter K, Fatka O, Hladil J, Kalvoda J, Šimůnek Z, Štorch P, Vašíček Z, Zajíc J, Zapletal J (2010) Outline of the geology of the Bohemian Massif. Czech Geological Survey, Praha

Chappel BW, Hine R (2006) The Cornubian Batholith: an example of magmatic fractionation on a crustal scale. Resour Geol 56:203–244

Cheng WR, Fontan F, Monchoux P (1992) Minéraux disséminés comme indicateurs du caractére pegmatitique du granite de Beauvoir, Massif d'Echassieres, Allier, France. Can Mineral 30:763–770

Claiborne LL, Miller CF, Walker BA, Wooden JL, Mazdab FK, Bea F (2006) Tracking magmatic processes through Zr/Hf ratios in rocks and Hf and Ti zoning in zircons: an example from the Spirit Mountain batholith, Nevada. Mineral Mag 70:517–543

Cobbing EJ, Pitfield PJ, Teoh LH (1986) The granites of the southeast Asian tin belt. J Geol Soc Lond 143:421–460

Erdmann S, Wodicka N, Jackson SE, Corrigan D (2013) Zircon textures and composition refractory recorders of magmatic volatile evolution? Contrib Mineral Petrol 165:45–71

Ewing RC, Meldrum A, Wang LM, Wang SX (2000) Radiation induced amorphization. In: Redfern SAT, Carpenter MA (eds) Transformation processes in minerals, Rev Mineral Geochem, vol 39. Chantilly, Mineral Soc Am, pp 319–361

Förster H-J (2006) Composition and origin of intermediate solid solutions in the system thorite-xenotime-zircon-coffinite. Lithos 88:35–55

Förster H-J, Ondrejka M, Uher P (2011) Mineralogical responses to subsolidus alteration of granitic rocks by oxidizing as-bearing fluids: REE arsenates and as-rich silicates from the Zinnwald granite, eastern Erzgebirge, Germany. Can Mineral 49:913–930

Förster H-J, Romer RL (2010) Carboniferous magmatism. In: Linneman U, Romer RL (eds) Pre-Mesozoic geology of Saxo-Thuringia – from the Cadomian active margin to the Variscan orogen. Schweizerbart, Stuttgart, pp 287–308

Förster H-J, Trumbull RB, Gottesmann B (1999) Late-collisional granites in the Variscan Erzgebirge, Germany. J Petrol 40:1613–1645

Gagnevin D, Daly JS, Kronz A (2010) Zircon texture and chemical composition as a guide to magmatic processes and mixing in a granitic environment and coeval volcanic system. Contrib Mineral Petrol 159:579–596

Geisler T, Pidgeon RT, Bronswijk W, Kurtz R (2002) Transport of uranium, thorium and lead in metamict zircon under low-temperature hydrothermal conditions. Chem Geol 191:141–154

Geisler T, Pidgeon RT, Kurtz R, Bronswijk W, Schleicher H (2003a) Experimental hydrothermal alteration of partially metamict zircon. Am Mineral 88:1496–1513

Geisler T, Rashwan AA, Rahn MKW, Poller U, Zwingmann H, Pidgeon RT, Schleicher H, Tomaschek F (2003b) Low-temperature hydrothermal alteration of natural metamict zircons from the Eastern Desert, Egypt. Mineral Mag 67:485–508

Govindaraju K (1994) Compilation of working values and sample description for 383 geostandards. Geostand Newslett 18:1–158

Grimes CB, Wooden JL, Cheudle MJ, John BE (2015) Fingerprinting tectono-magmatic provenance using trace elements in igneous zircon. Contrib Mineral Petrol 170:1–26

Hanchar JM, Hoskin PWO (eds; 2003) Zircon. Rev mineral Geochem, vol 53. Mineral Soc Am, Chantilly, 500 pp

Hoshino M, Kimata M, Nishida N, Shimizu M, Akasaka T (2010) Crystal chemistry of zircon from granitic rocks, Japan: genetic implications of HREE, U and Th enrichment. Neues Jb Mineral Abh 187:167–188

Hoskin PWO, Kinny PD, Wyborn D, Chapell BW (2000) Identifying accessory mineral saturation during differentiation in granitoid magmas: an integrated approach. J Petrol 41:365–1396

Hoskin PWO, Schaltegger U (2003) The composition of zircon and igneous and metamorphic petrogenesis. In: Hanchar JM, Hoskin PWO (eds) Zircon, Rev Mineral Geochem, vol 53. Chantilly, Mineral Soc Am, pp 27–62

Hoth K, Wasternack J, Berger HJ, Breiter K, Schovánek P (1995) Geologische Karte Erzgebirge-Vogtland 1:100 000. Sächsisches Landesamt für Umwelt, Landwirtschaft und Geologie, Freiberg

Huang XL, Wang RC, Chen XM, Hu H, Liu CS (2002) Vertical variations in the mineralogy of the Yichun topaz-lepidolite granite, Jiangxi province, southern China. Can Mineral 40:1047–1068

Irber W (1999) The lanthanide tetrad effect and its correlation with K/Rb, Eu/Eu*, Sr/Eu, Y/ho, and Zr/Hf of evolving peraluminous granite suites. Geochim Cosmochim Ac 63:489–508

Johan Z, Johan V (2005) Accessory minerals of the Cínovec (Zinnwald) granite cupola, Czech Republic: indicators of petrogenetic evolution. Mineral Petrol 83:113–150

Kempe U, Gruner T, Renno AD, Wolf D, René M (2004) Discussion on Wang et al. (2000) "chemistry of Hf-rich zircons from the Laoshan I- and A-type granites, Eastern China", mineral Magazin 64, 867–877. Mineral Mag 68:669–675

Kosterin AV, Shevaleevskii ID, Rybalova EK, Tolok KP (1963) Zr/Hf ratio in the zircons of some igneous rocks of Northern Kazakhstan. Geochemistry 1963:1007–1009

Linnemann U, Romer RL (2010) Pre-Mesozoic geology of Saxo-Thuringia – from the Cadomian active margin to the Variscan orogeny. Schweizerbart, Stuttgart, 488 p

Linnen RL, Cuney M (2005) Granite-related rare-element deposits and experimental constrains on Ta-Nb-W-Sn-Zr-Hf mineralization. Geol Assoc Canada Short Course Notes 17:45–68

Linnen RL, Keppler H (2002) Melt composition control of Zr/Hf fractionation in magmatic processes. Geochim Cosmochim Acta 66: 3293–3301

Lodders K (2010) Solar system abundances of the elements. In: Goswami A, Reddy BE (eds) Principles and perspectives in cosmochemistry, Lecture Notes of the Kodai school on 'Synthesis of elements in Stars' held at Kodaikanal observatory, India, April 29–May 13, vol 2008. Astrophysics and Space Science Proceedings, Springer, Berlin Heidelberg, pp 379–417

London D, Hervig RL, Morgan GBVI (1988) Melt-vapor solubilities and elemental partitioning in peraluminous granite-pegmatite system: experimental results with Macusani glass at 200 MPa. Contrib Mineral Petrol 99:360–373

Lyakhovich VV, Shevaleevskii ID (1962) Zr:Hf ratio in accessory zircons of granitoids. Geochemistry 1962:508–524

Merlet C (1994) An accurate computer correction program for quantitative electron probe microanalysis. Microchim Acta 114(115):363–376

Müller A, Breiter K, Seltmann R, Pécskay Z (2005) Quartz and feldspar zoning in the eastern Erzgebirge volcano-plutonic complex (Germany, Czech Republic): evidence of multiple magma mixing. Lithos 80:201–227

Müller A, Seltmann R, Halls C, Siebel W, Dulski P, Jeffries T, Spratt J, Kronz A (2006) The magmatic evolution of the Land's End pluton, Cornwall, and associated pre-enrichment of metals. Ore Geol Rev 28:329–367

Nardi LVS, Formoso MLL, Müller IF, Fontana E, Jarvis K, Lamarão C (2013) Zircon/rock partition coefficients of REEs, Y, Th, U, Nb, and Ta in granitic rocks: uses for provenance and mineral exploration purposes. Chem Geol 335:1–7

Nasdala L, Kronz A, Wirth R, Váczi T, Pérez-Soba C, Willner A, Kennedy AK (2009) The phenomenon of different electron microprobe totals in radiation-damaged and altered zircon. Geochim Cosmochim Acta 73:1637–1650

Palme H, O'Neill HSt (2004). Cosmochemical estimates of mantle composition. In: Carlson RW (ed) The mantle and core. Holland HD, Turrekian KK (executive eds) Treatise on Geochemistry, vol 2. Elsevier, pp 1–38

Patzer A, Pack A, Gerdes A (2010) Zirconium and hafnium in meteorites. Meteorit Planet Sci 45:1136–1151

Pupin JP (2000) Granite genesis related to geodynamics from Hf-Y in zircon. T RSE Earth 91:245–256

Raimbault L, Cuney M, Azencott C, Duthou JL, Joron JL (1995) Geochemical evidence for a multistage magmatic genesis of Ta-Sn-Li mineralization in the granite at Beauvoir, French Massif Central. Econ Geol 90:548–576

Rubatto D (2002) Zircon trace element geochemistry: partitioning with garnet and link between U-Pb ages and metamorphism. Chem Geol 184:123–138

Sawka WN (1988) REE and trace element variation in accessory minerals and hornblende from the strongly zoned McMurry Meadows pluton, California. T RSE Earth 79:157–168

Schmidt C, Rickers K, Wirth R, Nasdala L, Hanchar JM (2006) Low-temperature Zr mobility: an in situ synchrotron-radiation XRF study of the effect of radiation damage in zircon on the element release in H_2O+HCl±SiO_2 fluids. Am Mineral 91:1211–1215

Shannon RD (1976) Revised effective ionic radii and systematic studies of inter-atomic distances in halides and chalkogenides. Acta Crystallogr A 32:751–767

Štemprok M, Šulcek Z (1969) Geochemical profile through an ore-bearing lithium granite. Econ Geol 64:392–404

Taylor SR, McLennan SM (1995) The geochemical evolution of the continental crust. Rev Geophys 33:241–265

Tischendorf G (1989) Silicic magmatism and metalogenesis of the Erzgebirge. Veröffentlichungen Zentralinstitut für Physik der Erde, Potsdam 107:316 pp

Van Lichtervelde M, Holtz F, Dziony W, Ludwig T, Meyer H-P (2011) Incorporation mechanism of Ta and Nb in zircon and implications for pegmatitic systems. Am Mineral 96:1079–1089

Van Lichtervelde M, Melcher F, Wirth R (2009) Magmatic vs. hydrothermal origins for zircon associated with tantalum mineralization in the Tanco pegmatite, Manitoba, Canada. Am Mineral 94:439–450

Výravský J, Novák M, Škoda R (2017) Formation of pretulite ($ScPO_4$) by recrystallization of Sc-rich precursors in Dolní Bory pegmatite: evidence for different mobility of Sc, Y, REE and Zr in hydrothermal conditions. Chem Geol 449:30–40

Wang RC, Fontan F, Xu SJ, Chen XM, Monchoux P (1996) Hafnian zircon from the apical part of the Suzhou granite, China. Can Mineral 34:1001–1010

Wang X, Griffin WL, Chen J (2010) Hf contents and Zr/Hf ratios in granitic zircons. Geochem J 44:65–72

Wang RC, Zhao GT, Lu JJ, Chen XM, Xu SJ, Wang DZ (2000) Chemistry of Hf-rich zircons from the Laoshan I- and A-type granites, Eastern China. Mineral Mag 64:867–877

Wark DA, Miller CF (1993) Accessory mineral behavior during differentiation of a granite suite: monazite, xenotime and zircon in the Sweetwater wash pluton, southeastern California, U.S.A. Chem Geol 110:49–67

Wood SA (2005) The aqueous geochemistry of zirconium, hafnium, niobium and tantalum. Geol Assoc Canada Short Course Notes 17: 217–268

Yin R, Wang RC, Zhang AC, Hu H, Zhu JC, Rao C, Zhang H (2013) Extreme fractionation from zircon to hafnon in the Koktokay No.1 pegmatite, Altai, Northwestern China. Am Mineral 98:1714–1724

Zaraisky GP, Aksyuk AM, Devyatova VN, Udoratina OV, Chevychelov VY (2009) The Zr/Th ratio as a fractionation indicator of rare-metal granites. Petrology 17:25–45